REPORT NO. 243-034-11

LEVEL III

12

B's

AD A098162

ACOUSTICALLY SCANNED OPTICAL IMAGING DEVICES

Annual Technical Report

Principal Investigator:

G. S. Kino
(415) 497-0205

Sponsored by
Advanced Research Projects Agency
ARPA Order No. 2778

Contract No. N00014-76-C-0129

Edward L. Ginzton Laboratory
W. W. Hansen Laboratories of Physics
Stanford University
Stanford, California

ACOUSTICALLY SCANNED OPTICAL IMAGING DEVICES

Annual Technical Report

Principal Investigator:

G. S. Kino
(415) 497-0205

Sponsored by
Advanced Research Projects Agency
ARPA Order No. 2778

Contract No. N00014-76-C-0129
Program Code Number: 4D10
Contract Period: 1 October 1977 - 30 September 1980
Amount of Contract: $504,302.00
Form Approved, Budget Bureau - No. 22R0293

G. L. Report No. 3219

February 1981

Edward L. Ginzton Laboratory
W. W. Hansen Laboratories of Physics
Stanford University
Stanford, California

UNCLASSIFIED (18) ONR

SECURITY CLASSIFICATION OF THIS PAGE (When Data Entered)

REPORT DOCUMENTATION PAGE

READ INSTRUCTIONS BEFORE COMPLETING FORM

(19) 1. REPORT NUMBER: 243-834-11 ✓

2. GOVT ACCESSION NO.: AD-A098162

3. RECIPIENT'S CATALOG NUMBER:

4. TITLE (and Subtitle): (6) Acoustically Scanned Optical Imaging Devices

#10 = AF30739

5. TYPE OF REPORT & PERIOD COVERED: (9) Annual Technical Report, 1 July 1975-14 November 1980

6. PERFORMING ORG. REPORT NUMBER: (14) GL-3219

7. AUTHOR(s): (10) G.S. Kino, J. Bowers, R. Thornton, B. Khuri-Yakub

8. CONTRACT OR GRANT NUMBER(s): (15) N00014-76-C-0129, ARPA Order No. 2778

9. PERFORMING ORGANIZATION NAME AND ADDRESS:
Edward L. Ginzton Laboratory
W.W. Hansen Laboratories of Physics
Stanford University, Stanford, CA. 94305

10. PROGRAM ELEMENT, PROJECT, TASK AREA & WORK UNIT NUMBERS:
PE 61101E
8D10
Order No. 2778-5

11. CONTROLLING OFFICE NAME AND ADDRESS:
Defense Advanced Research Projects Agency
1400 Wilson Boulevard
Arlington, VA. 22209

12. REPORT DATE: (11) February 1981

13. NUMBER OF PAGES: 42 (12) 47

14. MONITORING AGENCY NAME & ADDRESS (if different from Controlling Office):
Office of Naval Research
Code 427
Arlington, VA. 22217

15. SECURITY CLASS. (of this report): Unclassified

15a. DECLASSIFICATION/DOWNGRADING SCHEDULE:

16. DISTRIBUTION STATEMENT (of this Report)

Approved for public release; distribution unlimited

17. DISTRIBUTION STATEMENT (of the abstract entered in Block 20, if different from Report)

18. SUPPLEMENTARY NOTES
ONR Scientific Office
(202) 696-4218

19. KEY WORDS (Continue on reverse side if necessary and identify by block number)
surface acoustic wave (SAW); storage correlator; convolver; acoustoelectric; silicon; gallium arsenide (GaAs); zinc oxide (ZnO); broad bandwidth; monolithic; adaptive filtering; echo suppression

20. ABSTRACT (Continue on reverse side if necessary and identify by block number)

A number of new ZnO based monolithic acoustoelectric devices have been demonstrated during the past three years, including Sezawa wave convolvers and storage correlators with 36 MHz bandwidth, Rayleigh wave Schottky diode and p-n diode storage correlators, and GaAs convolvers operating in a nonlinear resistive mode. These devices have been demonstrated in chirp and PSK compression experiments. A new, extremely fast SAW based adaptive filter was demonstrated in a variety of experiments, including echo suppression, spurious

DD FORM 1 JAN 73 1473 EDITION OF 1 NOV 65 IS OBSOLETE
S/N 0102-LF-014-6601

UNCLASSIFIED
SECURITY CLASSIFICATION OF THIS PAGE (When Data Entered)

20. (Abstract) signal suppression, and impulse response improvement of a bulk wave transducer. A reactive magnetron sputtering system was constructed, and the optimum deposition parameters were determined. ZnO films were deposited at extremely high rates (10 - 20 μm/hour), and excellent orientation is routinely obtained (FWHM of (0002) peak 5.3°).

TABLE OF CONTENTS

I. MANAGEMENT REPORT

A. Summary

During the last three years we have demonstrated GaAs acoustoelectric convolvers operating in a nonlinear resistive mode, Rayleigh wave ZnO/Si p-n diode and Schottky diode storage convolvers and storage correlators, and edge-bonded transducers. We have demonstrated monolithic Sezawa wave storage correlation with 36 MHz bandwidth, 32 dB input dynamic range, and 65 dB output dynamic range. A reactive magnetron sputtering system has been constructed and used to fabricate the above devices. The films have been extensively characterized and the optimum deposition parameters determined. Ghost cancellation, spurious signal suppression, and impulse response improvement of a bulk wave transducer have been demonstrated using a novel SAW storage correlator adaptive filter in which all calculations are performed inside the storage correlator without the need for an external microprocessor.

B. Research Plan

This is a final report on the present contract. A renewal contract is expected and we intend to continue our present work on the new contract. the main aim will be to demonstrate applications of the surface wave correlator as an adaptive filter to remove interfering echoes and distortion in nondestructive testing applications. For that purpose, we intend to build a reliable device with extremely low feedthrough signals, and we are aiming at a dynamic range of over 40 dBs and as near to 60 dBs as we can obtain.

C. Major Accomplishments

The major accomplishment on this program is the demonstration of a surface wave storage correlator adaptive filter in a monolithic configuration. We have demonstrated for the first time that by using a feedback loop, the device can be programmed to filter out distortion. We therefore believe that the device has great potential for removing ghost signals in television and for removing unwanted echoes and distortion in nondestructive testing, radar, and communications applications.

The second major accomplishment is to place the zinc oxide technology on a firm and reproducible footing. When we started this program, our zinc oxide devices and those of other laboratories were highly unreproducible. Now most of the devices work as predicted, and the zinc oxide always gives high coupling. We have also used a magnetron sputtering system with a zinc target. This makes it far easier to obtain a pure material for the target. Thus the system is much easier to use than the equivalent Japanese system employing a ZnO target.

D. Problems Encountered

None encountered.

E. Fiscal Status

Total amount of contract	$504,302
Expenditures & commitments through 11/14/80	$504,302
Estimated funds required to complete work	- 0 -
Estimated date of completion of work	14 November 1980

F. Action Required by DARPA/ONR

At the time of writing, we have still not received the renewal contract, although it has been approved by DARPA. This is causing serious financial problems and implies that the work, including the writing of reports, is going far slower than we would wish.

II. TECHNICAL PROGRESS REPORTS

A. ZnO Planar Magnetron Sputtering

During the last three years, a ZnO planar magnetron sputtering system was designed and built, and over 150 depositions have been made. The results from this system are much more reproducible than from the previous rf sputtering system, and better orientation of the ZnO layers has been achieved.

In the past six months, we have continued extensive characterization of the ZnO layers. Many of these results are included in Appendix C. The dependence of orientation (as measured by REDs) on substrate to target spacing is shown in Fig. 6. The dependence of orientation on substrate temperature is shown in Fig. 7. Clearly, the sputtering correlations for optimum orientation are a 500°C substrate temperature and 4.2 cm spacing. The resistivity of these layers is consistently extremely high (10^{10} Ωcm to 10^{12} Ωcm). Composition measurements do not show any impurities in the ZnO layer down to the EDAX detection limit.

B. Adaptive Filtering

A major application of SAW storage correlators has been the implementation of a SAW storage correlator based adaptive filter. The adaptive filter was used for echo cancelling[8] and to improve the impulse response of a bulk wave transducer.[9] These results have been summarized in the literature[8,9] and in past progress reports.[10] The main feature is very fast adaptation rates, typically 100 - 500 μs and good supression (10 - 15 dB) of echoes and other distortions. The main limitation was the narrow bandwidth (8 MHz) of the ZnO/Si Rayleigh wave device used in the

experiment. This work is being repeated with our broadband Sezawa wave storage correlator.

C. GaAs Convolver and Edge-Bonded Transducers

A problem with ZnO/Si devices which was consistently encountered during the previous contract was the deposition of reproducibly oriented ZnO layers on SiO_2 in the interaction region. The use of GaAs as a substrate eliminates this problem since GaAs is weakly piezoelectric and ZnO would not be needed in the interaction region.

GaAs convolvers with ZnO on the ends for higher coupling to interdigital transducers (IDTs) were constructed (see Fig. 1). These devices had high efficiency (-62 dBm) due to the use of the nonlinear resistive characteristic of a diode. This was the first demonstration of a nonlinear SAW device which used the nonlinear resistive component. All other SAW convolvers use the nonlinear capacitance effect.

The SAW coupling coefficient for ZnO/GaAs devices is low and even lower for GaAs alone. This results in narrow bandwidth devices. To obtain broad bandwidth devices on GaAs, an attractive alternative to IDTs is the use of Edge Bonded Transducers (EBTs) (Fig. 2). With the use of EBTs, 100 MHz should be achievable, and ZnO would not be needed at all on the device. A number of EBTs were fabricated, and a theory of EBTs was developed.[1] These transducers worked well for center frequencies below 50 MHz ; however, in spite of manufacturers claims, we were unable to obtain a piezoelectric ceramic which would work at 100 MHz or more without being excessively lossy.

At the same time, a planar magnetron ZnO sputtering system was designed, constructed, and extensively tested[2] (see next section). With this new

system, high quality oriented ZnO layers on SiO_2 were reproducibly obtained, and all of our effort was shifted to ZnO/Si devices.

D. Comparison of Approaches: Bandwidth Loss Calculation

A series of calculation were made[3] which compared the potential bandwidth obtainable from $LiNbO_3$ airgap devices, ZnO/Si Rayleigh wave devices, and ZnO/Si Sezawa wave devices. The results are given in Fig. 3 which shows the bandwidth loss relationship for each of these devices. As expected, $LiNbO_3$ IDTs are much better than ZnO/Si Rayleigh wave devices. However, the use of the Sezawa mode in ZnO/Si is just as good as $LiNbO_3$ and has the advantage of being capable of integration with other integrated circuit devices on the silicon chip.

E. Sezawa Wave pn Diode Storage Correlators

Sezawa wave delay lines with 42 MHz bandwidth and 18 dB loss were fabricated.[4,5] Sezawa wave convolvers with high efficiency (-50 dBm) were constructed and demonstrated. Sezawa wave storage correlators with an efficiency of -60 dBm were constructed and demonstrated in chirp and Barker code compressions during the last six month period.[6] The details of this work are presented in Appendix A. With appropriate tuning networks, 37 MHz bandwidth (25% bandwidth) as a storage correlator has been achieved.[5] This is over 4 times as large as the bandwidth attained with our Rayleigh wave ZnO/Si correlators and is a comparable performance to $LiNbO_3$ devices operating at the same center frequency.

F. Schottky Diode Storage Correlators

In our initial efforts at making ZnO/Si storage correlators, we have used pn diodes as the storage elements. Their advantage is the relative ease with which they are fabricated. Their major disadvantage is the fact that 1 μs charging pulses are needed to fully charge up pn diodes. This means that the efficiency of a pn diode correlator will fall rapidly when one tries to store modulated signals that have a data rate faster than 1 MHz .

In order to eliminate this problem we have developed Schottky diode storage correlators. We have demonstrated the ability of a Schottky diode correlator to store efficiently using a pulse width of 1 ns ,[7] thus making the ZnO/Si transducer bandwidth the limiting bandwidth as opposed to tahe diode response characteristic. The details of this work are included in Appendix B.

The Schottky diode correlators we have constructed to date are efficient (-64 dBm) and have good storage times (10 msec) . Combining the use of Schottky diodes with Sezawa mode transducers, we expect soon to be able to demonstrate very efficient 40 MHz bandwidth devices in spread spectrum and adaptive filtering experiments.

G. Large Area Devices

In the past, each SAW device has been made individually. We have begun processing arrays of devices. A photo of a 4 cm x 4 cm ZnO/Si wafer viewed under green light is shown in Fig. 4. As can be seen, a problem we have encountered is uniformity of the thickness of the ZnO layer. A new target has been constructed which should improve the thickness uniformity by a factor of 5 . We are encouraged by the fact that the P.E.D. measurements indicate excellent orientation uniformity across the entire wafer. A photo of a water

of 70 Sezawa wave waveguided convolvers is shown in Fig. 5. More testing of this wafer is needed to determine yield and device performance.

References

1. J. E. Bowers, B. T. Khuri-Yakub, G. S. Kino, and F. Yu, "Design and Application of High Efficiency Wideband SAW Edge-Bonded Transducers," Proc. Ultrasonics Symposium, p. 794, 1978.
2. B. T. Khuri-Yakub and J. G. Smits, "Reactive Magnetron Sputtering of ZnO," Proc. Ultrasonics Symposium, 1980.
3. G. S. Kino, J. Bowers, B. Khuri-Yakub, and R. Thornton, "Acoustically Scanned Optical Imaging Devices," Technical Progress Report for Office of Naval Research, August 1980.
4. J. E. Bowers, Ph.D. dissertation, Stanford University, 1981.
5. J. E. Bowers, B. T. Khuri-Yakub, and G. S. Kino, "Broadband Efficient Thin Film Sezawa Wave Interdigital Transducers," Appl. Phys. Lett., vol. 10, p. 806, 1980.
6. J. E. Bowers, B. T. Khuri-Yakub, and G. S. Kino, "Monolithic Sezawa Wave Storage Correlators and Convolvers," Proc. Ultrasonics Symposium, 1980.
7. R. L. Thornton and G. S. Kino, "Monolithic Schottky Diode Storage Correlator," Proc. Ultrasonics Symposium, 1980.
8. D. Behar, G. S. Kino, J. E. Bowers, and H. Olaisen, "Storage Correlator as an Adaptive Inverse Filter," Electr. Lett., vol. 16, p. 130, 1980.
9. J. E. Bowers, G. S. Kino, and D. Behar, "Adaptive Deconvolution Using a SAW Storage Correlator," IEEE Trans. Sonics and Ultrasonics, to be published.
10. G. S. Kino, J. Bowers, B. Khuri-Yakub, and R. Thornton, "Acoustically Scanned Optical Imaging Devices," Technical Progress Report for Office of Naval Research, February 1980.

Figure Captions

1. Schematic drawing of a GaAs storage correlator.
2. Schematic drawing of an edge-bonded transducer.
3. Theoretical minimum loss obtainable as a function of bandwidth based on Ref. 3.
4. Photo of a 4 cm x 4 cm silicon substrate with 8 μm of ZnO viewed under green light.
5. Photo of a wafer of 70 Sezawa wave waveguided convolvers.
6. RED measurements of ZnO layers grown at different spacings.
7. RED measurements of ZnO layers grown at different temperatures.

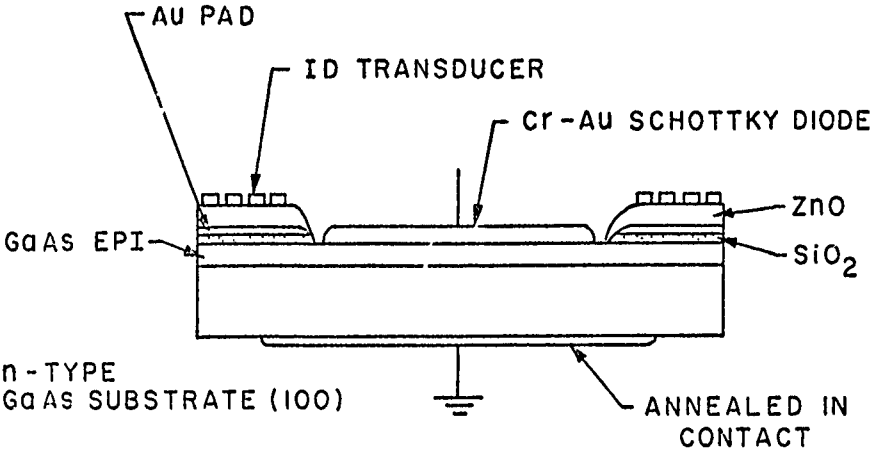

DRAWING OF GaAs MONOLITHIC CONVOLVER

Figure 1

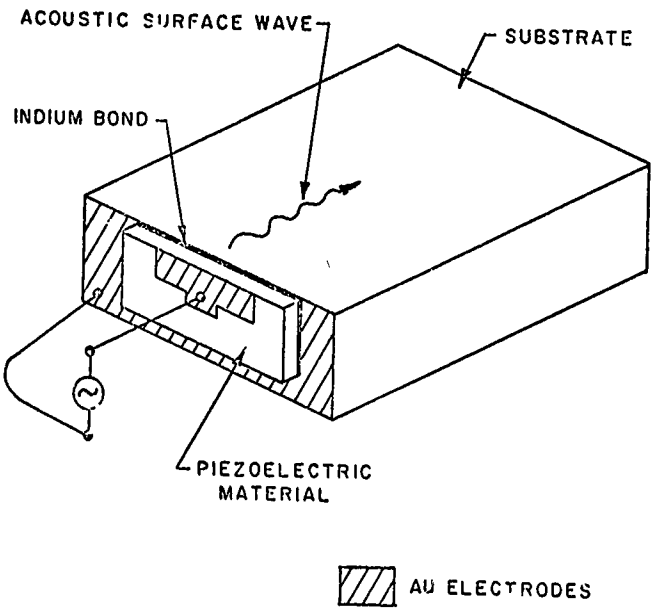

AN EDGE BONDED TRANSDUCER

Figure 2

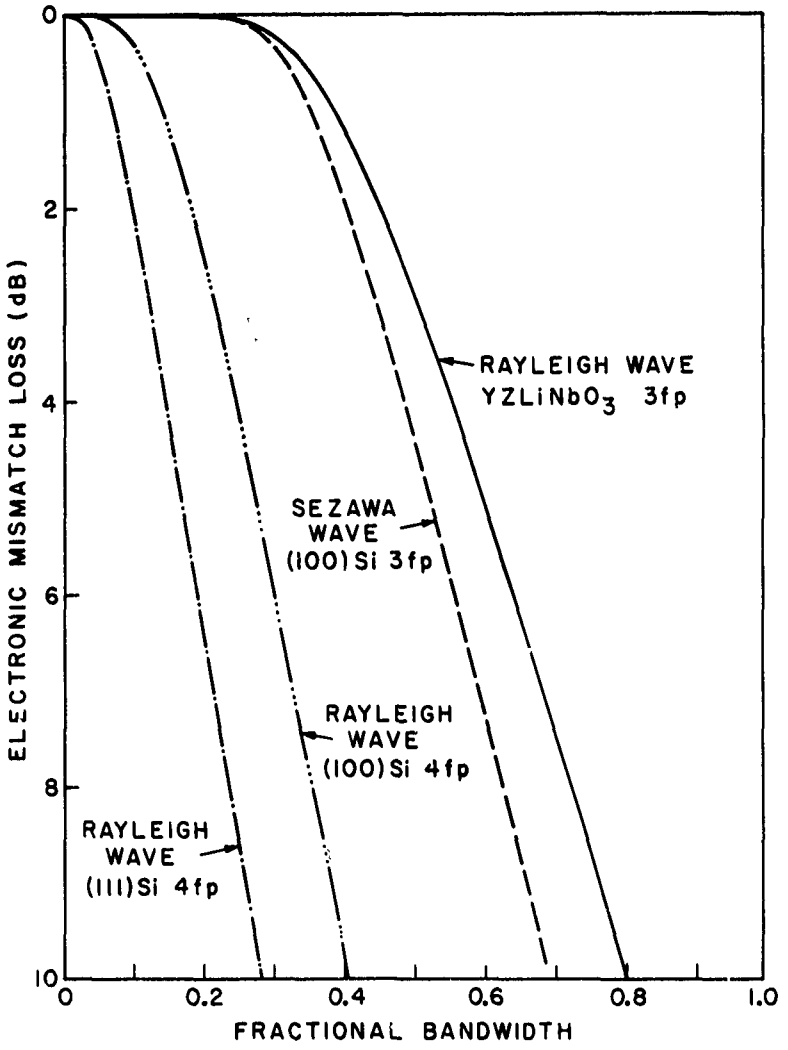
ELECTRONIC MISMATCH LOSS (dB)
0
2
4
6
8
10
0
0.2
0.4
0.6
0.8
1.0
FRACTIONAL BANDWIDTH
RAYLEIGH WAVE
YZLiNbO3 3fp
SEZAWA
WAVE
(100)Si 3fp
RAYLEIGH
WAVE
(100)Si 4fp
RAYLEIGH
WAVE
(111)Si 4fp

FIGURE 3

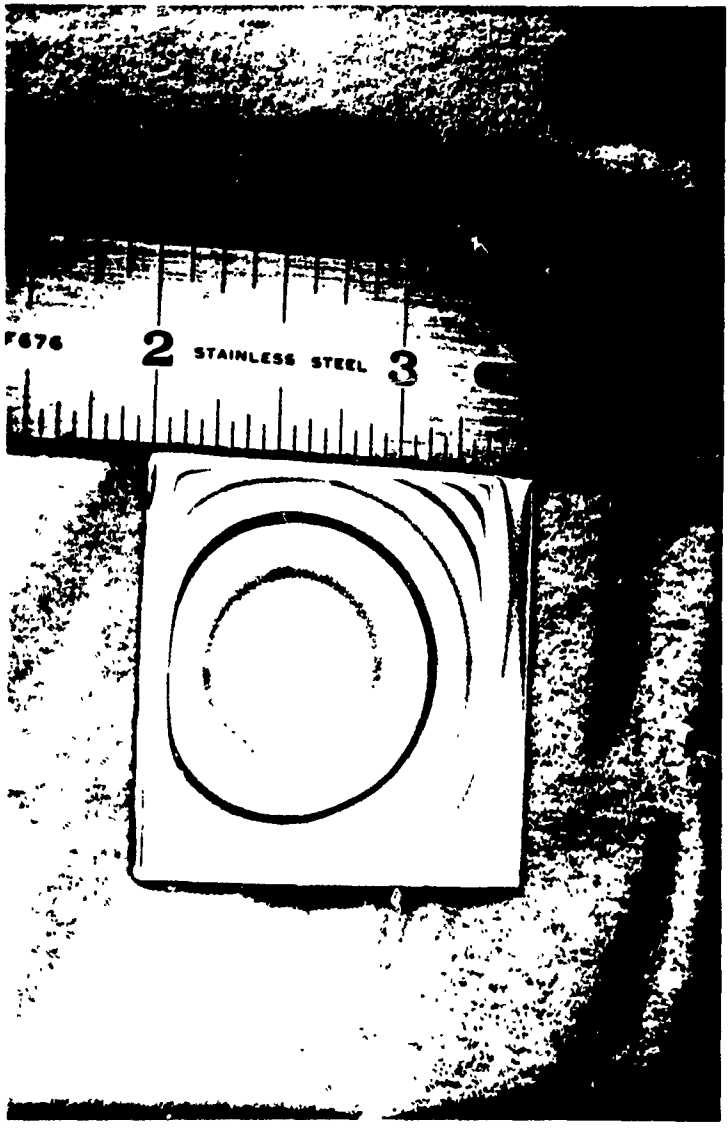

FIGURE 4

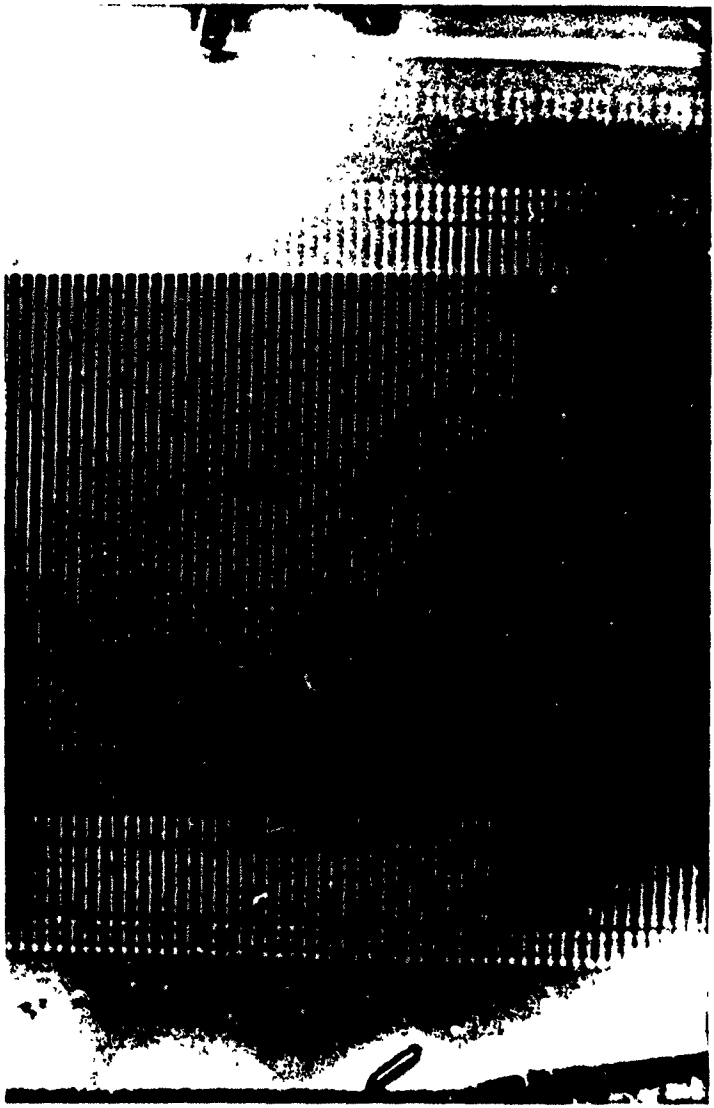

FIGURE 5

Dependence of Orientation on Substrate-Target Spacing

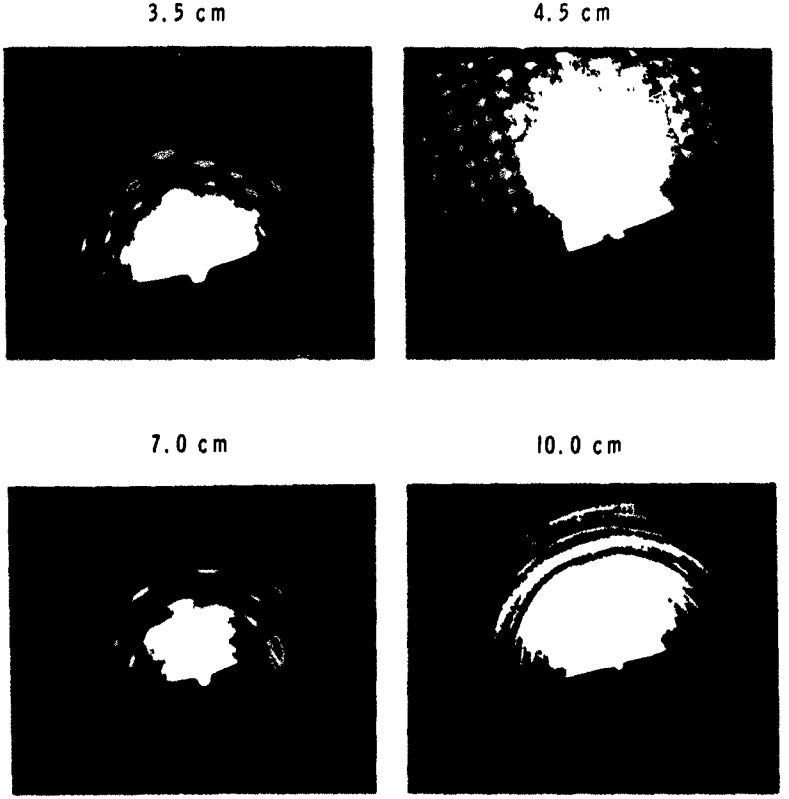

FIGURE 6

(a) NO HEATER, 25-220 °C
(4.5 cm SPACING)

(b) 500 °C
(4.5 cm SPACING)

(c) 450 °C
(5cm SPACING)

(d) 600 °C
(7cm SPACING)

FIGURE 7

List of Publications

1. G.S. Kino, "A Review of Some Possible Applications of Acoustic Convolver Technology," invited paper, Proc. Reunion International Organisee par la DRME, Paris, France, April 1976.
2. G.S. Kino, "Acoustoelectric Interactions in Acoustic Surface Wave Devices," invited paper, Proc. IEEE, vol. 64, no. 5, pp. 724-748, May 1976.
3. P. Borden,B.T. Khuri-Yakub, H.C. Tuan, and G.S. Kino, "ZnO Convolver Development," Proc. Ultrasonic Symposium, Annapolis, Maryland, September 1976.
4. P. Borden and G.S. Kino, "Input Correlation with the ASW Storage Correlator," Electr. Lett., vol. 13, no. 16, pp. 470-471, 4 August 1977.
5. P. Borden and G.S. Kino, "The Charging Process in the Acoustic Surface Wave p-n Diode Storage Correlator," Appl. Phys. Lett., vol. 31, no. 8, pp. 488-490, 15 October 1977.
6. P.G. Borden and G.S. Kino, "An Analytic Theory for the Storage Correlator," Proc. Ultrasonic Symposium, Phoenix, Arizona, October 1977.
7. H.C. Tuan and G.S. Kino, "A New Zinc Oxide on Silicon Monolithic Storage Correlator," Proc. Ultrasonic Symposium, Phoenix, Arizona, October 1977.
8. H.C. Tuan and G.S. Kino, "A Monolithic Zinc Oxide on Silicon p-n Diode Storage Correlator," Appl. Phys. Lett., vol. 31, no. 10, pp. 641-643, 15 November 1977.
9. H.C. Tuan and G.S. Kino, "Large Time Bandwidth Product Correlation and Holographic Storage with an ASW Storage Correlator," Electr. Lett., vol. 13, pp. 709-710, 24 November 1977.

10. C.S. DeSilets, A.R. Selfridge, and G.S. Kino, "Highly Efficient Transducer Arrays Useful in Nondestructive Testing Applications," Proc. Ultrasonic Symposium, Cherry Hill, New Jersey, September 1978.

11. H.C. Tuan, P.M. Grant, and G.S. Kino, "Theory and Application of Zinc-Oxide-on-Silicon Monolithic Storage Correlators," Proc. Ultrasonic Symposium, Cherry Hill, New Jersey, September 1978.

12. J.E. Bowers, B.T. Khuri-Yakub, G.S. Kino, and K-Y Yu, "Design and Applications of High Efficiency Wideband SAW Edge Bonded Transducers," Proc. Ultrasonic Symposium, Cherry Hill, New Jersey, September 1978.

13. P.M. Grant and G.S. Kino, "Adaptive Filter Based on SAW Monolithic Storage Correlator," Electr. Lett., vol. 14, no. 17, pp. 562-564, 17 August 1978.

14. D. Behar, G.S. Kino, J.E. Bowers, and H. Olaisen, "Storage Correlator as an Adaptive Inverse Filter," Electr. Lett., vol. 16, no. 4, pp. 130-131, 14 February 1980.

15. G.S. Kino, "Zinc Oxide on Silicon Acoustoelectric Devices," invited paper, Proc. Ultrasonic Symposium, New Orleans, Louisiana, September 1979.

16. J.E. Bowers, B.T. Khuri-Yakub, and G.S. Kino, "Broadband Efficient Thin-Film Sezawa Wave Interdigital Transducers," Appl. Phys. Lett., vol. 36, no. 10, 15 May 1980.

17. J.E. Bowers, G.S. Kino, D. Behar, and H. Olaisen, "Adaptive Deconvolution Using an ASW Storage Correlator," submitted to Special Issue of IEEE Trans. on Sonics and Ultrasonics, May 1980.

18. H.C. Tuan, J.E. Bowers, and G.S. Kino, "Theoretical and Experimental Results for Monolithic SAW Memory Correlators," Proc. IEEE Trans. Sonics and Ultrasonics, vol. SU-27, no. 6, pp. 360-369, November 1980.

19. G.S. Kino, "Signal Processing with the Storage Correlator," invited paper, SPIE 24th Annual Technical Symposium, San Diego, California, July 1980.

20. J.E. Bowers, B.T. Khuri-Yakub, and G.S. Kino, "Monolithic Sezawa Wave Storage Correlators and Convolvers," Proc. Ultrasonic Symposium, Boston, Massachusetts, November 1980.

21. R.L. Thornton and G.S. Kino, "Monolithic ZnO on Si Schottky Diode Storage Correlator," Proc. Ultrasonic Symposium, Boston, Massachusetts, November 1980.

22. C.H. Chou, J.E. Bowers, A.R. Selfridge, B.T. Khuri-Yakub, and G.S. Kino, "The Design of Broadband and Efficient Bulk Wave Transducers," Proc. Ultrasonic Symposium, Boston, Massachusetts, November 1980.

23. B.T. Khuri-Yakub and J. Smits, "Reactive Magnetron Sputtering of ZnO," Proc. Ultrasonic Symposium, Boston, Massachusetts, November 1980.

APPENDIX A

MONOLITHIC SEZAWA WAVE STORAGE CORRELATORS AND CONVOLVERS

J.E. Bowers, B.T. Khuri-Yakub, and G.S. Kino

Edward L. Ginzton Laboratory
Stanford University
Stanford, California 94305

Abstract

Monolithic Sezawa wave convolvers with an efficiency of -50 dBm and a bandwidth of 25 MHz are demonstrated in a number of Barker code and chirp compression experiments. Extensive data is presented on a monolithic Sezawa wave storage correlator with an external correlation efficiency of -63 dBm and a bandwidth of 32 MHz . The input dynamic range is 30 dB , and the output is linearly related to the readout voltage over a range of 75 dB . Analytic and experimental results on the effect of dispersion on correlation, input correlation, and convolution are presented. It is found that dispersion in Sezawa wave convolvers with 2 cm interaction regions limits the usable bandwidth to 25 MHz . The variation of group velocity with frequency was measured over a 70 MHz range of frequencies and found to be in good agreement with theoretical predictions.

1. Introduction

Surface acoustic wave (SAW) convolvers and storage correlators have been made using a monolithic, thin film approach (typically ZnO/Si)[1,2] or hybrid arrangements where a piezoelectric substrate is pressed against a semiconductor.[3,4] The monolithic approach has the advantages of ruggedness, smaller size, fewer spurious signals, and potentially lower cost. Unfortunately, these devices have had narrow bandwidths (5 to 20 MHz , depending on the design and electronic mismatch loss[5]) due to the small coupling coefficient of the first $\Delta v/v$ peak of the first Rayleigh mode in ZnO/Si devices. The Sezawa mode (second Rayleigh mode) has a much higher coupling coefficient[6,7] and fractional bandwidths as large as those obtained with $LiNbO_3$ devices are theoretically possible.[5]

Gunshor and co-workers[8,9] have fabricated Sezawa wave convolvers and storage correlators with bandwidths of 13% and with external efficiencies of -57 dBm and -103 dBm , respectively. In this paper, we present results on Sezawa wave convolvers and storage correlators with bandwidths of 21% and external efficiencies of -50 dBm and -63 dBm, respectively. The results of Barker code and chirp compression experiments are also presented, and data on the dependence of the output voltage on the acoustic and read voltages range is given. The problem of dispersion in these devices is experimentally and theoretically examined.

2. Experimental Considerations

A schematic drawing of a monolithic storage correlator is shown in Fig. 1. The biggest difference between the Rayleigh wave and Sezawa wave versions of this device is the thickness of the ZnO layer: 8.3 μm for the Sezawa mode device and 1.2 μm for the Rayleigh mode device for operation at 165 MHz . The devices are batch processed using (100) n-type 5 - 10 Ωcm silicon wafers. A boron diffusion was used to form the diodes in the storage correlator. The convolver used in the experiments below has the same device configuration as shown in Fig. 1 except that there are no p-n diodes. The ZnO layer was sputter-deposited at 500°C using a planar magnetron sputtering system.[10] The ZnO thickness (8.3 μm) was chosen for maximum Sezawa wave coupling for (100) Si substrates.[7] Four finger pair interdigital transducers (IDTs) with a 1 mm beamwidth were used.

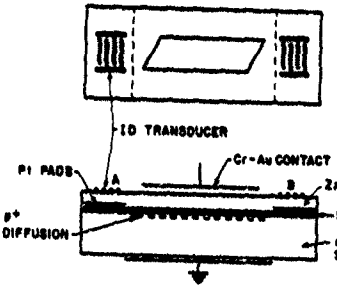

Figure 1 - Cross-sectional drawing of a monolithic SAW storage correlator

For the storage correlator in the plate to acoustic readout mode, a signal is applied to the center or top plate port to read out the signal stored in the diode array. The ends of the top plate generate spurious surface waves, unless the ends are slanted (Fig. 2a) or configured in some other manner to reduce the spurious waves received

Reprinted from 1980 ULTRASONICS SYMPOSIUM PROCEEDINGS, November 1980

0090-5607/80/0000-0118 $00.75 © 1980 IEEE

by the IDT. However, this causes a phase distortion across the beam since the SAW velocity in the metallized region is different from the unmetallized region. This distortion is negligible for Rayleigh wave devices. However, for Sezawa waves, the SAW coupling coefficient is much higher ($\Delta v/v = .028$), and a phase distortion of 135° occurs for a beamwidth of 1 mm (30 wavelengths) and a slant of 25°. Consequently, a configuration such as that shown in Fig. 2b was used to eliminate phase distortion but still reduce spurious SAW generation.

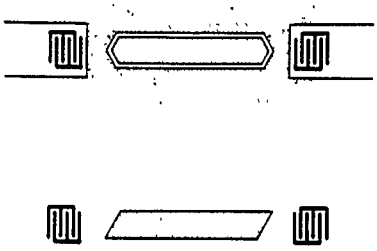

Figure 2 - Top plate metallization used for (a) Rayleigh wave storage correlators, and (b) Sezawa wave storage correlators

Another problem associated with the use of Sezawa waves and four finger pair IDTs is the generation and detection of bulk acoustic waves. This problem can severely limit the dynamic range. However, by bonding the back of the substrate to a brass carrier box with indium solder, the amplitude of these waves has been reproducibly reduced by more than 40 dB. The acoustic impedances of silicon, and brass are 13.7×10^6 and 31×10^6 kgs/m^2, respectively, and consequently, after a number of reflections at the back surface, essentially all of the bulk wave energy is coupled into the carrier box.

This technique also ensures that the device is well grounded, and this reduces problems with direct electromagnetic pick-up between the different ports of the device. The direct pick-up can be reduced below the level of the other spurious signals through appropriate shielding and grounding techniques. A storage correlator mounted in a well shielded box is shown in Fig. 3.

3. Results and Discussion

A. Sezawa Wave Convolvers

Results from Sezawa wave convolvers will be presented in this section. Storage correlator results will be presented in the next section, and a consideration of the dispersion problems in these devices will be presented in the final section.

Monolithic Sezawa wave convolvers with an efficiency of -50 dBm at 155 MHz have been fabricated. This is a higher efficiency than has been reported for monolithic Rayleigh wave convolvers.[1] The efficiency of Rayleigh wave waveguided devices is slightly higher than the Sezawa wave convolver[11] and it is expected that the efficiency of waveguided Sezawa wave convolvers would be even higher. The 3 dB convolution efficiency bandwidth was 25 MHz with the use of 3-element tuning circuits on each port. Bandwidths of 40 MHz are obtainable with the use of more elaborate tuning circuits and slightly greater mismatch losses.[5]

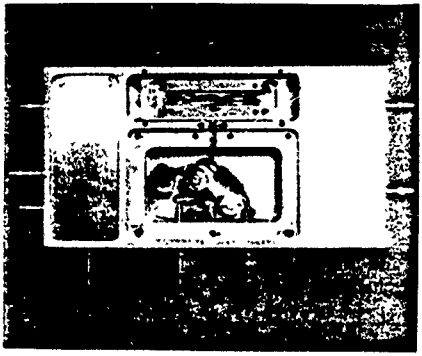

Figure 3 - Photo of a storage correlator and the box containing tuning networks. The top plate tuning network is shown. Access to the acoustic matching network is through the bottom of the box.

The results of 5 and 11 bit Barker code pulse compressions are shown in Figs. 4a and 4b, respectively. The good dynamic range and uniformity are evident from this figure. No problems with dispersion were evident, even when bit rates of 10 MHz were used.

A series of chirp correlation experiments were performed to see if dispersion would limit the usable time-bandwidth product of these devices. The experiments used 3 μs long chirp signals of variable bandwidths up to a maximum of 25 MHz bandwidth. To avoid pulse broadening due to the nonlinearity of the chirp frequency variation with time, one chirp generator was used, and its output was mixed with 2 cw signals to generate the necessary up and down chirp signals. Using the input 25 MHz chirp shown in Fig. 5a, the compressed output pulse is shown in Figs. 5b and 5c. The 4 dB pulse width is 44 ns, and the total pulse compression is 68. The theoretical compression is 3×25 or 69. The sidelobes are not as small as theoretically expected, nor are they symmetric about the central peak. This is due to the fact that (1) the variation of chirp frequency with time is not linear, and 2) the amplitude of different frequency components of the input chirp varies by as much as 2 dB (Fig. 5a).

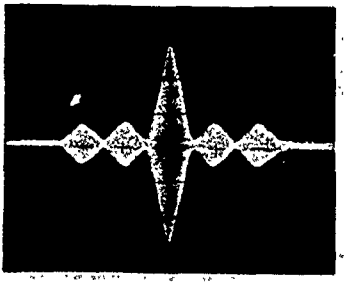

(a) 0.5 μs/div

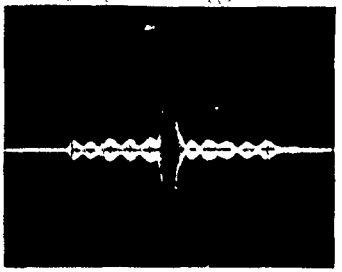

(b) 0.5 μs/div

Figure 4 - Barker code pulse compression using a 25 MHz Sezawa wave convolver. (a) 5 bit code; (b) 11 bit code

The fact that the output pulse width is not significantly limited by dispersion is a remarkable result. The variation in group delay over the 23 MHz bandwidth is .2 μs. Thus, one might expect the minimum output pulse width to be of this order and the maximum time bandwidth product for this device to be 30. However, it is shown in the final section that dispersion limits Sezawa wave convolvers to a usable time bandwidth product of roughly 80.

b. Sezawa Wave Storage Correlators

Monolithic Sezawa wave storage correlators have been fabricated with an external correlation efficiency of -63 dBm when all three ports have been tuned to 50 Ω. The convolution efficiency of this device was -56 dBm. When broadband tuning circuits (Fig. 1) were used, the correlation efficiency decreased by 3 dB, and the bandwidth was 32 MHz (Fig. 6). All of the following results were obtained using the broadband version of this device. The plate-to-acoustic readout[4] mode was used in each case.

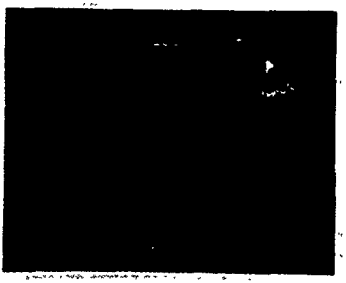

(a) 5 MHz/div

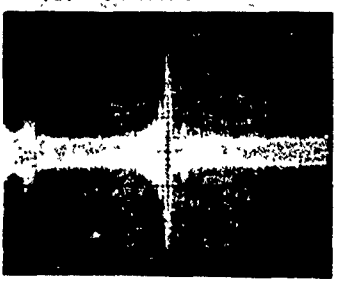

(b) 0.2 μs/div

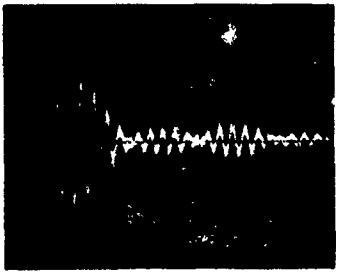

(c) 0.02 μs/div

Figure 5 - Chirp compression experiment. (a) Frequency spectrum of input chirp; (b) and (c) Output pulse

The correlation of two square pulses is shown in Fig. 7. The input dynamic range of this device is 30 dB, i.e. the triangle peak is 30 dB above the largest spurious signal. The dependence of the correlation output voltage on acoustic voltage is shown in Fig. 8 as a function of the input acoustic voltage. The dependence is linear over 32 dB.

The dynamic range is limited on the upper end by the diode saturation.[12] The dynamic range is limited on the lower end by spurious surface waves excited by the readout signal at the top plate. The spurious signals are predominantly generated by defects in the ZnO layer.[13] The amplitude of these spurious signals is proportional to the amplitude of the readout signal. Hence, the output dynamic range is much larger. This is illustrated in Fig. 9, where the dependence of the output correlation power on the readout power is given. The range over which the output power is linearly related to the readout power is 75 dB. There are a number of applications where this large output dynamic range can be exploited. For instance, in adaptive filtering,[14] the filter transfer characteristic is stored in the device, and then it is desirable to use the filter in situations where the power level of the filter input (readout signal) may vary over a large range. This device is ideally suited for that purpose.

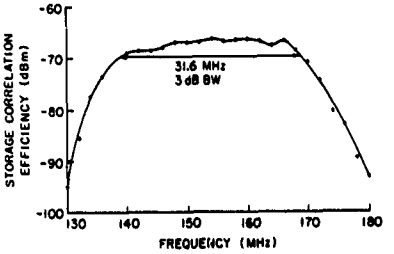

Figure 6 - Dependence of storage correlation efficiency on frequency.

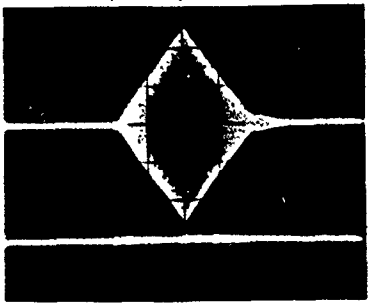

Figure 7 - Upper trace: Storage correlation of two square pulses
Lower trace: Spurious signals generated by the readout pulse (2 μs/div).
V_A = 10 V, V_W = 5 V, V_R = 1 V,
t_A = 3.9 μs, t_N = .5 μs, t_R = 3.9 μs

The storage correlation of two 5 bit Barker codes is shown in Fig. 10. The acoustic signal was modulated with one Barker code and stored with a 100 ns write pulse. The other Barker code was carried on the readout signal. This technique has a larger signal-to-spurious level than if the correlation of two Barker codes is stored in the device and read out with a 100 ns pulse. The reason is that the readout signal excites a number of spurious signal sources, and the different 3 μs spurious signals interfere with each other.

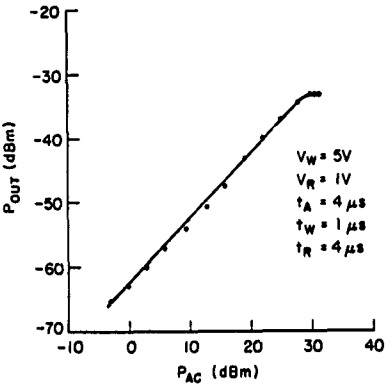

Figure 8 - Dependence of the output correlation power on the acoustic power P_A

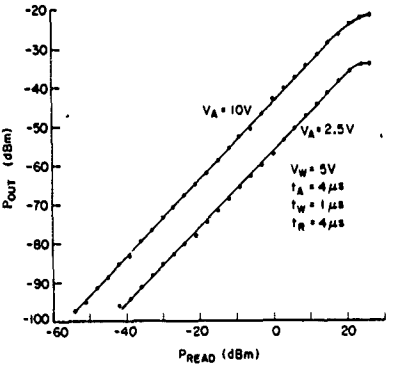

Figure 9 - Dependence of the output correlation power on the readout power P_R for two acoustic voltages and 3 MHz bandwidth

A number of different chirp correlation experiments were performed. In one case, a chirp is stored in the device with a 50 ns storing pulse on the plate port. Another chirp was applied to the plate port and the output taken from the acoustic port opposite the input acoustic port. 5, 10, 20, and 28 MHz chirps were used, and the 4 dB pulse width was slightly larger than the theoretical

width in each case. The discrepancy was largest for the 25 MHz chirp where the output 4 dB pulse width was 50 ns rather than the theoretical (no dispersion) value of 36 ns .

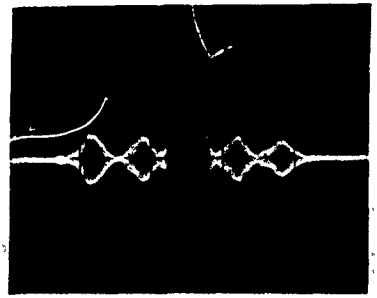

Figure 10 - The storage correlation of a 5 bit Barker code

In another chirp experiment, two 20 MHz , 100 μs long chirps were input correlated, and the output read with a 50 ns pulse. The output pulse 4 dB width at the input transducer was 100 μs , yielding a pulse compression of 1000 . Note, however, that the theoretical (no dispersion) compression is 3 times larger. The output at the opposite transducer was 200 μs wide, yielding a pulse compression of only 500 .

c. Effects of Dispersion

Any SAW device that utilizes a layered substrate will be dispersive, and the degree of dispersion is minimized when the SAW velocities of the layer and substrate are almost equal. Unfortunately, the SAW velocity of ZnO (2639 m/s) is significantly smaller than the SAW velocity of silicon (4920 m/s). Dispersion causes phase distortion of the wave and can thus limit the usable bandwidth to much less than the IDT bandwidth.

The amount of dispersion depends on the slope of the group velocity curve. The group and phase velocities for Rayleigh waves and Sezawa waves (Fig. 11) are shown for the ZnO(100)Si structure. The slope of the group velocity curve is small at the position of the second peak in Δv/v for Rayleigh waves; however, the slope is significant for Sezawa wave devices and for Rayleigh wave devices using the first Δv/v peak. The Sezawa wave group velocity in an 8 μm ZnO/(100)Si device was measured and is shown in Fig. 11. The experimental and theoretical results are in good agreement except for a constant overall factor of -95 .

The analytic effects of dispersion in a convolver have been treated by Morgan.[15] He found that the convolution output of a dispersive convolver is the convolution of (1) the output in the absence of dispersion with (2) a complex chirp function whose time constant is

$$\tau = \left| \frac{2L}{V_G^2} \frac{dV_G}{d\omega} \right|_{\omega = \omega_0}$$

where L is the length of the interaction region. For the Sezawa wave convolver considered, $\tau = .038$ μs . Consequently, the maximum usable bandwidth is of the order of 25 MHz . Morgan's analysis[15] is applicable to amplitude modulated signals such as the Barker code compression experiments discussed earlier. For chirp compression, an analysis of the phase distortion reveals that for 25 MHz chirps, the pulse width should broaden to 50 ns for a ZnO/Si Sezawa wave convolver with an interaction length of 1.6 cm . Thus, the convolver experimental results where an output pulse width of 44 ns and a time bandwidth product of 68 was obtained probably represent an upper limit to the usable time bandwidth product.

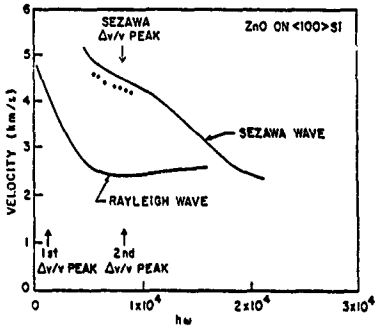

Figure 11 - Dependence of group velocities on normalized frequency hω . h is the ZnO film thickness for the ZnO/(100)Si system

There are a number of ways to use the storage correlator in a pulse compression application. Eight ways to correlate two codes are shown in Fig. 12. There are eight additional ways that two codes can be convolved which are equivalent to the eight listed in Fig. 12.

Consider one particular mode of operation (underlined in Fig. 12) where one code is sent into the acoustic port (A) and stored, and a second code is sent into acoustic port A to readout the correlation. Both codes undergo the same distortion, and the correlation peak is not significantly broadened. Using an analysis similar to Morgan's[15] the output is $V_{out} = V_0 * \text{sinc}^2(t/\tau)$ where V_0 is the output for no dispersion, * stands for convolution, and $\tau^{-1} = \omega_0 + V_{G0}/(dV_G/d\omega)_{\omega 0}$. For a Sezawa wave device, $\tau = 1.75 \times 10^{-13}$ s , so the distortion is negligible. Note however, that unlike a convolver, attenuation will affect the output, and pulse broadening can occur. For instance, if up chirps are used, the high frequency end travels the farthest, and the high frequency

components of both chirps are decreased, which for significant amounts of attenuation results in pulse broadening. This is not a significant problem in our devices when the frequencies are in the 100 to 200 MHz range and travel lengths of several centimeters. However, this places a limit on the maximum time bandwidth product. The loss in ZnO increases as f^2 and is roughly 10 dB/cm at 300 MHz[16], so a time bandwidth product of 1000 is definitely an upper limit for monolithic ZnO/Si storage correlators.

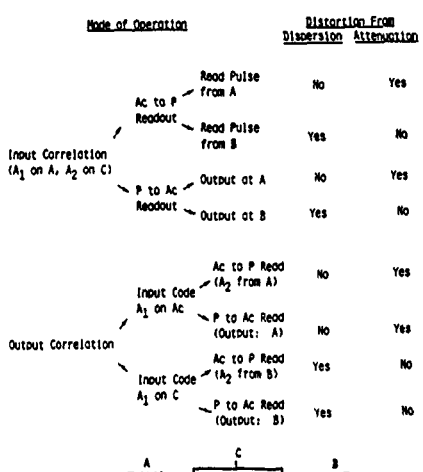

Figure 12 - Effects of dispersion and attenuation on the different modes of operation

From Fig. 12, we see that any time the storage correlator is used as a two-port device, dispersion is not a problem, but attenuation might be a problem. If all three ports are used, the opposite is true This would explain the storage correlator experimental result given above that for identical inputs, the time bandwidth product was 500 for three port operation and 1000 for two port operation.

4 Conclusions

Broadband, efficient Sezawa wave convolvers and correlators have been demonstrated in a number of experiments. It was shown that dispersion does not limit the usable time bandwidth product for convolvers where TB is less than 70 , and that this is in agreement with predictions based on group velocity data. The effect of dispersion on the usable time bandwidth product for storage correlators depends on the mode of operation, and with the optimum modes, much larger time bandwidth products may be obtained than with monolithic convolvers

Acknowledgement

The authors wish to thank J.B. Green and R.L. Thornton for many valuable discussions on this topic.

This work was supported by the Defense Advanced Research Projects Agency and monitored by the Office of Naval Research under Contract N00014-76-C-0219.

References

1. B.T. Khuri-Yakub and G.S. Kino, "A Detailed Theory of the Monolithic Zinc Oxide on Silicon Convolver," IEEE Trans. Sonics/Ultrasonics, vol. 24, p. 34, 1977.
2. H.C. Tuan, B.T. Khuri-Yakub, and G.S. Kino, "A New Zinc Oxide on Silicon Monolithic Storage Correlator," Proc. Ultrasonics Symposium, p. 496, 1977.
3. K.A. Ingebrigtsen, R.A. Cohen, and R.W. Mountain "A Schottky Diode Acoustic Memory and Correlator," Appl. Phys. Lett., vol. 26, p. 596, 1975.
4. P.G. Borden and G.S. Kino, "An Analytic Theory for the Storage Correlator," Proc. Ultrasonics Symposium, p. 485, 1977.
5. J.E. Bowers, "A Technique for Calculating the Bandwidth-Loss Relationship for Acoustic Transducers," submitted to J. Acous. Soc. Am., October 1980.
6. G.A. Armstrong and S. Crampin, "Piezoelectric Surface Waves in Zinc-Oxide-Layered Substrates," Electr. Lett., vol. 9, p. 322, 1973.
7. J.E. Bowers, B.T. Khuri-Yakub, and G.S. Kino, "Broadband Efficient Thin-Film Sezawa Wave Interdigital Transducers," Appl. Phys. Lett., vol. 36, p. 806, 1980.
8. J.K. Elliot, R.L. Gunshor, R.F. Pierret, and A.R. Day, "A Wideband SAW Convolver Utilizing Sezawa Waves in the Metal-ZnO-SiO_2-Si Configuration," Appl. Phys. Lett., vol. 32, p. 515, 1978
9. F.C. Lo, R.L. Gunshor, and R.F. Pierret, "Monolithic (ZnO) Sezawa-Mode pn-Diode-Array Memory Correlator," Appl. Phys. Lett., vol. 39, p. 725, 1979.
10. B.T. Khuri-Yakub and J.G. Smits, "Reactive Magnetron Sputtering of ZnO," Proc. Ultrasonics Symposium, 1980.
11. J.B. Green and B.T. Khuri-Yakub, "A 100 μm Beamwidth ZnO on Si Convolver," Proc. Ultrasonics Symposium, p. 911, 1979.
12. H.C. Tuan, J.E. Bowers, and G.S. Kino, "Theoretical and Experimental Results for Monolithic SAW Memory Caorrelators," IEEE Trans. Sonics/Ultrasonics, to be published November 1980.
13. H C. Tuan, "The Monolithic ZnO on Silicon Storage Correlator," Ph.D Thesis, Stanford University, October 1980.
14. J.E. Bowers, G.S. Kino, D. Behar, and H. Olaisen, "Adaptive Deconvolution Using a SAW Storage Correlator," IEEE Trans. Sonics/Ultrasonics, to be published December 1980.
15. D P. Morgan, "Effect of Dispersion in Surface Acoustic Wave Convolvers," IEEE Trans. Sonics/Ultrasonics, vol. SU-22, p. 274, 1975.
16. J. deKlerk, R.W Weinert, and B.R. McAvoy, "SAW Attenuation in Hydrothermally Grown ZnO," Proc. Ultrasonics Symposium, p. 667, 1978.

APPENDIX B

MONOLITHIC ZnO ON Si SCHOTTKY DIODE STORAGE CORRELATOR

R. L. Thornton and G. S. Kino

Edward L. Ginzton Laboratory
Stanford University
Stanford, California 94305

Abstract

In this paper, we describe a monolithic Schottky diode ASW storage correlator. The device is fabricated using the ZnO on Si technology, with the ZnO film being deposited by sputter deposition in an rf magnetron discharge system.

The device operates on the first order Rayleigh mode at a frequency of 125 MHz and employs a ZnO film 1.6 μm in thickness, with 1000 Å of sputter deposited SiO_2 between the diode array and the ZnO.

Using PtSi Schottky barrier diodes as the storage elements, it is possible to store a signal efficiently within a single rf cycle. This is a major improvement over the pn diode configuration, which needs 10 to 100 rf cycles for efficient storage.

The device has a convolution efficiency of -60 dBm and a correlation efficiency of -64 dBm when operated in the acoustic to plate readout mode.

1. Introduction

The monolithic storage correlator is a device that has received a good deal of attention in recent years,[1,2,3] and the theory of operation for the device has been explored in some detail.[3,4] In the past, the dominant structure for such devices has used p-n diodes as the storage elements. P-N diodes have finite recombination times for injected minority carriers which are usually longer than the duration of one rf cycle. For this reason, it is almost always necessary to use read-in signals of several rf cycles duration in order to reach the point at which the efficiency of the device saturates.

In this report, we describe a monolithic storage correlator fabricated using Schottky diodes as the storage elements. Since Schottky diodes are majority carrier devices, they are "faster" than p-n diodes in the sense that they are not recombination time limited and can therefore be made to reach saturation within a single rf cycle. This gives Schottky diode devices an advantage over p-n diode devices in applications requiring high resolution waveform storage.

The Schottky diode correlator described here was fabricated by employing the ZnO on Si structure, first used successfully in the fabrication of convolvers and p-n diode correlators.[1,5] The device has demonstrated its ability to store a waveform within a single rf cycle and with an efficiency comparable to that of p-n diode correlators. It has the important advantage over the equivalent air-gap device that the input voltage required on the plate to turn on the diodes is almost 2 orders of magnitude lower, and no pre-charging signal is required.

2. Fabrication Process

The device shown in Fig. 1 was fabricated on 10 Ω-cm <111> silicon using platinum silicide as the metallization for the Schottky barriers. Platinum silicide is particularly well-suited to this purpose for several reasons.

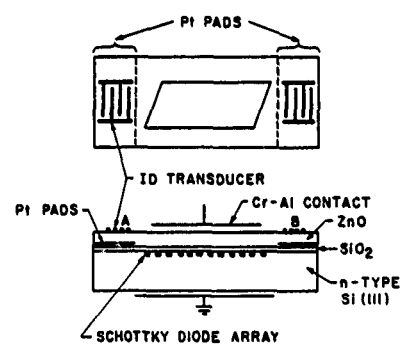

Figure 1 - Schematic diagram of monolithic Schottky diode storage correlator

First of all, the PtSi technology can produce self-aligning diode structures, making it possible to fabricate diode arrays with 4 μm spacing. This is done by etching the required windows in an oxide layer that has been thermally grown to 1000 Å,

depositing platinum over the entire wafer, and annealing at 460°C for 10 minutes. Platinum reacts with silicon to form platinum silicide in the areas where it is in contact with the silicon, but the SiO_2 acts as a barrier to the reaction everywhere else. All that is left then is to etch away the remaining free platinum, leaving behind the platinum silicide Schottky barriers.

The second reason for the desirability of PtSi has to do with the fact that it forms one of the highest known barrier heights to n-type silicon, on the order of .86 volts, and therefore will provide lower leakage currents and longer storage times than most other Schottky diodes on silicon.

The third and perhaps most important reason for the use of the platinum silicide has to do with the fact that the platinum silicide film formed is stable up to about 900°C . This is essential because of the necessity to heat the entire device to temperatures on the order of 500°C in order to perform the ZnO deposition which will be discussed later. Many other metals that form Schottky barriers to silicon, such as aluminum and gold, deteriorate into undesirable alloys or doped contacts at these temperatures.

Once the Schottky barriers are formed, they are covered with an insulating layer of sputter-deposited SiO_2 , the purpose of which is to provide a high quality insulator between the diodes and the metal top-plate. The ZnO film itself provides a large degree of insulation, having resistivities typically in the range of 10^{10} to 10^{12} Ω-cm . The lower end of this resistivity range, however, corresponds to a maximum storage time of 10 ms , in which case the leaky ZnO would limit the storage time in the device. The SiO_2 layer ensures that the limitation on storage time is due only to the diode leakage.

It has been found that the process of depositing the SiO_2 layer can produce a drastic shift in the threshold voltage of the MOS diodes in the region between the Schottky diodes.[6] Depending on the polarity of this charge, the surface of the silicon can be driven either into accumulation or inversion. Inversion must be strictly avoided as it will result in very large leakage currents. Both directions of drift are undesirable in the sense that they can result in having to apply large (and perhaps unattainable) bias voltages to the device in order to reach the flatband or partially depleted region, where the convolution or correlation efficiency will be greatest.

We have found that annealing sputter-deposited SiO_2 in forming gas for approximately two hours can result in a drastic improvement in the C-V characteristic of the devices. Figure 2a shows the C-V characteristic of a film with 1000Å of sputtered SiO_2 before annealing, and Fig. 2b shows that same film after annealing. Note not only the factor of 2 reduction in threshold voltage but also the reduction in the area of the mobile ion hysteresis loop. We have also observed very dramatic increases in diode reverse leakage currents after sputtering SiO_2, followed by equally dramatic reductions in leakage currents after the annealing process. Both of these experiments tend to indicate that the problem is indeed one of charge trapped in the oxide layer.

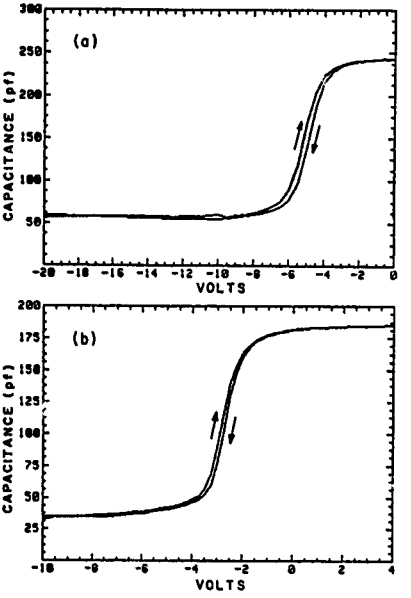

Figure 2 - Typical C-V characteristics of gold sputtered SiO_2-thermal SiO_2-silicon MOS capacitor (a) before and (b) after annealing for two hours in forming gas. Note change in scale between the two graphs and significant shift in threshold voltage after annealing

The ZnO deposition process is carried out in an rf magnetron sputtering station. Detailed characterization of the deposition parameters in this station is covered elsewhere in these conference proceedings.[7] Typical deposition parameters for the process involve heating the substrates to a temperature of 450°C in a 7 micron oxygen atmosphere and sputtering with an rf power of 1.25 kw .

We have performed experiments to determine the effect of the ZnO sputter-deposition on the leakage currents in our Schottky barrier diodes. These experiments indicate that the deterioration of diode quality due to ZnO deposition is relatively small, manifesting itself in a slight lowering of barrier height from .86 ± 01 volts to .85 ± .01 volts. Moreover, these shifts are observed

independent of whether or not the diode measured is physically shielded from the plasma or not.

These two results can be explained very well by the supposition that ZnO bombardment damage is not so much a factor in the slight lowering in barrier height as is the activation of impurities piled up at the PtSi-Si interface.

It has been observed that when PtSi is formed by thermal annealing of Pt on Si, the impurity dopants in the consumed silicon will tend to be excluded from the PtSi and will "pile up" at the PtSi-Si interface.[8,9] At an annealing temperature in the PtSi formation furnace of 460°C , the annealing time of 10 minutes is not sufficient to fully activate these impurities electronically. Therefore when the samples are placed in the ZnO deposition system at 450°C for typically one to two hours, the piled up impurities are electronically activated and begin to contribute to barrier lowering. Thus, the heating in the deposition station is a more significant factor than the plasma when one considers deterioration of the diodes, but the deterioration is not so severe as to make the diodes unusable.

After the sputter deposition of the ZnO, metallization for top-plates and transducers is performed using standard photolithographic techniques.

Figure 3 is a photograph of a device completely fabricated and ready for bonding of the transducers and packaging for operation.

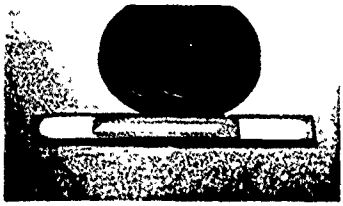

Figure 3 - Monolithic Schottky diode storage correlator ready for bonding and packaging.

3. Device Operation

We have fabricated Schottky diode correlators using the above procedure in order to demonstrate the fast storage properties of Schottky diodes in a monolithic structure.

The device operates at a center frequency of 122 MHz . The acoustic wavelength is 32 μm at the center frequency, and the interdigital transducers are 10 finger pairs in length. In order to maximize the first order Rayleigh mode coupling, the thickness of the ZnO film was 1.6 μm . The diode array consisted of diodes 4 μm in width with an inter-diode spacing of 4 μm . The width of the acoustic transducers and the diode array were both 1 mm .

In first characterizing this device, its performance as a delay line and convolver were measured, and it was found that the insertion loss was 24 dB , and the convolution efficiency was -60.5 dBm .

In order to investigate the properties of the device as a correlator, an acoustic to top-plate readout mode experiment was set up, as shown in Fig. 4. The acoustic stored waveform and acoustic readout waveform are ~3 μs in length, corresponding to the length of the top-plate. The storing pulse on the top-plate was 1 nS in width, which is small when compared to one rf cycle, which is 8 nS in duration.

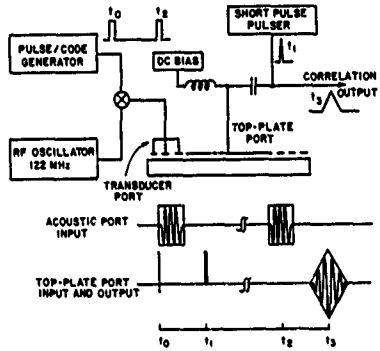

Figure 4 - Set up for acoustic to plate readout experiment $t_1 = t_0 + 4$ μs , $t_2 = t_0 + (20$ μm to storage time) , $t_3 = t_2 + 4$ μs

Figure 5 shows the output on the top-plate when both acoustic waveforms are rectangles. From the peak height of the triangle output, we conclude that we have a correlation efficiency of -64 dBm . This is close to the best efficiency ever reported for a ZnO on silicon storage correlator[10] with the exception of waveguided correlators.[11] The good linearity of the sides of the triangle in Fig. 5 indicates that the correlation interaction is also quite uniform over the length of the device.

The output correlation is a strong function of applied top-plate pulse amplitude only over a small range of top-plate pulse amplitudes. Figure 6 shows the measured dependence of the acoustic output voltage on the amplitude of a 4 nS pulse. It can be seen that the "threshold" for efficient storage is about 2 volts, and above this threshold the output slowly decreases when the pulse height is further increased. This voltage is almost 2 orders of magnitude smaller than the voltage required to produce similar operation in the $LiNbO_3$ separate medium Schottky diode correlator.[12]

We have varied the width of the storing pulse and have found that the correlation efficiency is

a strong function of both the width of the storing pulse and the exact shape of the pulse at its peak. The maximum efficiency for this device occurs when the storing pulse is as short as our setup would allow, on the order of 1 nS . This observation leads us to the conclusion that the recombination time effects which are symptomatic of the p-n diode correlator are indeed negligible in the Schottky diode correlator at these frequencies.

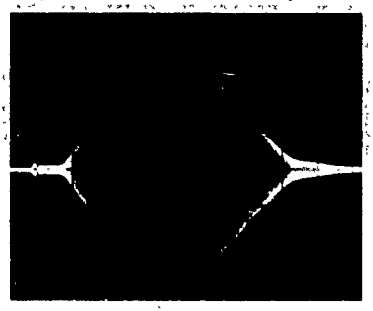

Figure 5 - Autocorrelation of two square pulses ~3 μs in length , 1 μs/div

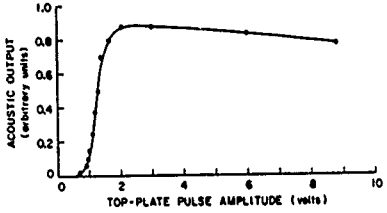

Figure 6 - Relative correlation output versus pulse amplitude of a 4 nS top-plate storing pulse

We have also measured the storage time of this device. Figure 7 shows the output of the device when a rectangular waveform is stored and an extremely wide readout pulse of greater than 20 ms duration is used. In this experiment there was no DC bias on the top-plate. We can see the envelope of the decay in the amplitude of the output correlation and can conclude that the 3 dB decay storage time of the device is 7.5 ms , although after 14 msec , the output correlation is still more than 25 dB above the noise level.

We have observed this storage time to be dependent on the DC bias applied to the top-plate, with positive bias increasing the storage time and negative bias decreasing it. This is indeed bias dependence we should expect, since negative bias tends to invert the surface, making the surface p type with its corresponding very low barrier height of .25 volt.

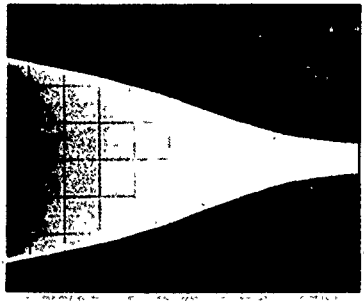

Figure 7 - Decay envelope of correlation output demonstrating storage time of device. 2 ms/div

To demonstrate the ability of this device to perform correlations of more complicated waveforms, we have set up experiments with various bi-phase codes. First in Fig. 8, is the autocorrelation of a 7 bit Barker code, which does show the theoretical sidelobe suppression level and pulse compression ratio, with some feedthrough. In Fig. 9, we have the autocorrelation of a 5 bit alternating phase bitstream. Also in this photograph the individual lobes are in agreement with their theoretical form, and the signal is produced with maximum device efficiency. These experiments would be possible with a p-n diode correlator only if the storing pulse were narrowed to prevent smearing of the output waveform, which would result in a significant reduction in efficiency for typical p-n diode correlator configurations.

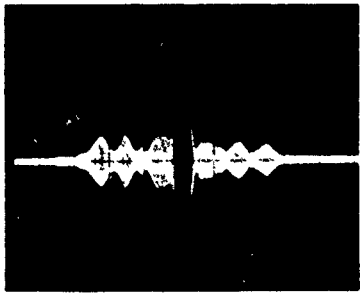

Figure 8 - Autocorrelation of a 7 bit Barker code 1 μsec/div

4. Conclusions

In conclusion, we note that we have designed and successfully fabricated a monolithic Schottky diode storage correlator. The device exhibits a correlation efficiency of -64 dBm , which compares favorably with the most efficient non-waveguided ZnO on Si correlator.

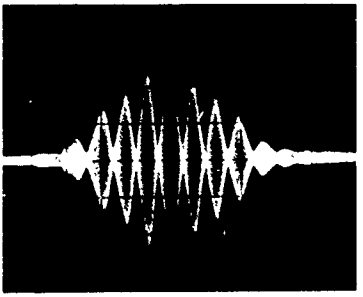

Figure 9 - Autocorrelation of a 5 bit + - + - + code bitstream. 1 μsec/div

We have demonstrated the ability of this device to acquire an exact copy of an rf waveform within one rf cycle in this highly efficient manner and to do so with a storage time of at least 7.5 ms .

Acknowledgements

The authors are grateful to B. Fank and J. Berenz of Varian Associates for use of their thin film deposition facilities. We would also like to acknowledge useful discussions with J. Bowers, J. Green, and B. T. Khuri-Yakub. This work was supported by the Defense Advanced Research Projects Agency and monitored by the Office of Naval Research under Contract N00014-76-C-0129.

References

1. H.C. Tuan and G.S. Kino, "A Monolithic Zinc Oxide on Silicon p-n Diode Storage Correlator," Appl. Phys. Lett., vol. 31, no. 10, 15 November 1977.

2. F.C. Lo, R.L. Gunshor, and R.F. Pierret, "Monolithic (ZnO) Sezawa Mode p-n Diode Array Memory Correlator," Appl. Phys. Lett., vol. 34, no. 11, 1 June 1972.

3. H.C. Tuan, P.M. Grant, and G.S. Kino, "Theory and Application of Zinc Oxide on Silicon Monolithic Storage Correlators," Proc. Ultrasonics Symposium, ...

4. H.C. Tuan, J.E. Bowers, and G.S. Kino, "Theoretical and Experimental Results for Monolithic SAW Memory Correlators," IEEE Trans. on Sonics and Ultrasonics, to be published November 1980.

5. B.T. Khuri-Yakub and G.S. Kino, "A Monolithic Zinc Oxide on Silicon Convolver," Appl. Phys. Lett., vol. 25, no. 4, 15 August 1974.

6. S.Y. Wu and N.P. Formigoni, "Charge Phenomena in DC Reactively Sputtered SiO_2 Films," J. Appl. Phys., vol. 39, no. 12, November 1968.

7. B.T. Khuri-Yakub and J. Smits, "Reactive Magnetron Sputtering of ZnO," Proc. Ultrasonics Symposium, 1980.

8. H. Muta, "Electrical Properties of Platinum-Silicon Contact Annealed in an H_2 Ambient," Jpn. J. Appl. Phys., vol. 17, no. 6, June 1978.

9. J.B. Bindell, W.M. Moller, and E.F. Labuda, "Ion-Implanted Low Barrier PtSi Schottky Barrier Diodes," IEEE Trans. on Electr. Dev., vol. ED-27, no. 2, February 1980.

10. J.E. Bowers, B.T. Khuri-Yakub, and G.S. Kino, "Monolithic Sezawa Wave Storage Correlators and Convolvers," Proc. Ultrasonics Symposium, 1980.

11. J.B. Green, B.T. Khuri-Yakub, and G.S. Kino, "A New Narrow Beamwidth High Efficiency Zinc Oxide on Silicon Storage Correlator," J. Appl. Phys., to be published January 1981.

12. P.G. Borden and G.S. Kino, "An Analytic Theory for the Storage Correlator," Proc. Ultrasonics Symposium, 1977.

APPENDIX C

REACTIVE MAGNETRON SPUTTERING OF ZnO

B. T. Khuri-Yakub and J. G. Smits

Edward L. Ginzton Laboratory
Stanford University
Stanford, California 94305

Abstract

A planar magnetron system is used to sputter zinc oxide on a variety of substrates. A zinc target is used, and sputtering is done in an oxygen atmosphere. The zinc oxide films are evaluated by bulk and surface acoustic measurements, scanning electron microscopy, reflection electron diffraction, x-ray diffraction, surface roughness, etching rate, and resistivity measurements. Zinc oxide films are grown on a variety of substrates such as gold, aluminum, platinum, and oxidized (111) and (100) silicon. Highly oriented films are obtained on all the substrates with a typical standard deviation in the rocking curves of the order of 0.2 - 0.5° . Typical sputtering parameters are: rf power = 1 - 1.25 kw , sputtering rate = 10 - 20 μm per hour, oxygen partial pressure = 5 - 7 μm , substrate temperature = 450 - 500°C, and target-to-substrate spacing = 4 - 7 cm .

In the last two to three years, planar magnetron systems have been used to sputter well oriented (c-axis normal) zinc oxide (ZnO) films on a variety of substrates.[1,2] Planar magnetron sputtering offers several advantages over the usual diode or triade sputtering. Namely, the sputtering rates are higher, and the process control is easier because electron bombardment of the substrate is reduced, thus allowing for better control of the substrate temperature.[3]

In this work, we use a planar magnetron system with a zinc target and carry out the sputtering in an oxygen atmosphere. A schematic diagram of the sputtering head is shown in Fig. 1. The additional advantages gained in such a system are: first, the zinc and oxygen used can be more pure than a ZnO target, and second, the zinc target has a better thermal conduction than a zinc oxide target. Thus, larger amounts of rf power can be supplied, which gives a still higher sputtering rate.

The quality of the ZnO films is determined by using x-ray diffraction, x-ray rocking curve, reflection electron diffraction, scanning electron microscopy, resistivity, surface roughness, etching rate, and acoustic measurements.

ZnO films were sputtered on gold, aluminum, platinum, fused quartz, thermally oxidized (111) silicon, thermally oxidized (100) silicon, and thermally oxidized p^+ regions in (100) silicon. These substrates are used for a variety of bulk wave and surface wave devices.

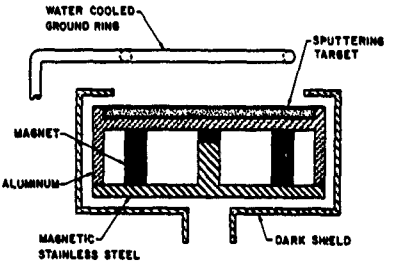

Figure 1 - Schematic diagram of the planar magnetron sputtering head.

Typical sputtering conditions are: oxygen pressure = 5 - 7 μm , substrate temperature = 450 - 500°C , target-to-substrate spacing = 4 - 7 cm , rf power = 1 - 1.25 kw , magnetic field strengh = 150 G , and a sputtering rate of 10 - 20 μm per hour. The best ZnO films obtained to date were deposited under the following conditions: oxygen pressure = 7 μm , substrate temperature = 500°C , target-to-substrate spacing = 4.2 cm , rf power = 1.25 kw , and a sputtering rate of 18 μm per hour. Table 1 shows an x-ray profile of the quality of the films obtained for such a set of sputtering conditions on the various substrates used. Included in Table 1 is an x-ray profile of a naturally occurring single crystal piece of ZnO (Zincite).

The x-ray measurement of Zincite is used as a calibration of our diffractometer and as a reference for our sputtered films. It is seen in Table 1 that the standard deviation in the rocking curve of Zincite is $\sigma_{r.c.} = .21°$, and the full width at half maximum (FWHM) of the (0002) and (0004) peaks is 15° The x-ray profile of Zincite is used as a measure of instrumental broadening. Assuming that the x-ray diffractometer traces are Gaussian, the x-ray profile of Zincite should be subtracted from that of the sputtered films to obtain their true profile. The quality of the ZnO films on Al and Pt is not as good as the quality of the films on

the other substrates because both metal films were not well oriented. We conclude that well oriented metal back electrodes are necessary for the growth of well oriented ZnO films. Figure 2 shows an x-ray diffractometer result from a 4 μm ZnO film grown under optimum deposition conditions on oxidized (111) silicon. Note that the Cu-kα_1 and Cu-kα_2 lines are clearly split. Figure 3 shows an x-ray rocking curve result of the film in Fig. 2. It is seen from the x-ray results that the sputtered ZnO films have an excellent orientation with the c-axis normal to the surface of the substrate.

Table 1

X-ray profile of ZnO films deposited under optimum conditions

Substrate	FWHM (0002)	FWHM (0004)	$\frac{I(0004)}{I(0002)}$ %	$\sigma°_{r.c.}$
Al	0.31	0.75	10.9	1.10
Au	0.19	0.50	7.5	0.47
Pt	0.24	0.55	8.6	0.94
SiO_2 Si (111)	0.19	0.45	9.75	0.52
SiO_2 Si (100)	0.37	0.65	8.4	0.76
Zincite	0.19	0.19	17.0	0.21

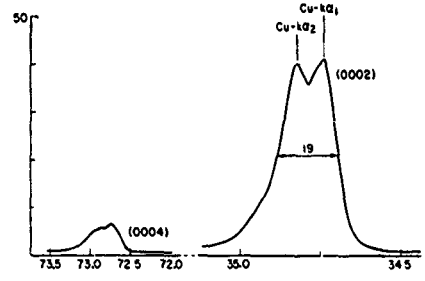

Figure 2 - X-ray diffraction trace of a c-axis normal ZnO film on a SiO_2/Si substrate.

Figure 4 shows a reflection electron diffraction (RED) result of the film of Fig. 2. The spots in the RED pattern correspond to diffraction planes in the film. Note that the large number of spots observed and their sharpness are indicative of the excellent quality of the films obtained

Figure 5 shows a scanning electron microscope picture on a fracture edge for the film of Fig. 2. Again, the smooth texture of the growth is indicative of the high quality of the ZnO film.[4]

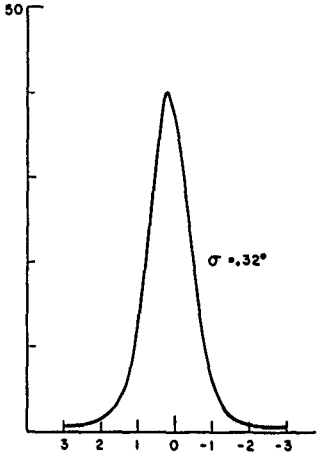

Figure 3 - X-rocking curve of the (0002) plane of the ZnO film in Fig. 2.

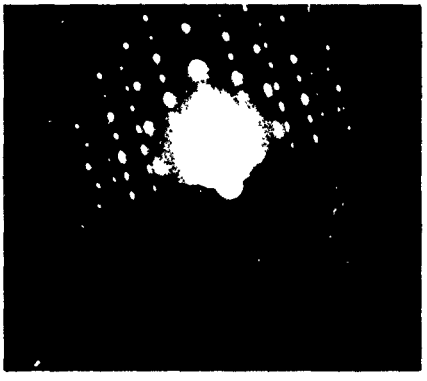

Figure 4 - Reflection electron diffraction pattern of the ZnO film in Fig. 2.

The dc resistivity of the ZnO films grown under all sputtering conditions was measured, and the value of the resistivity ranged from 10^{10} to 10^{12} ohm-cm This high value of resistivity makes our ZnO film very suitable for acoustic device applications.

ZnO films were etched in a CH_3COOH H_3PO_4 H_2O solution in the proportion of 1:x:1 For $x \leq 10^{-5}$, the etching rate was constant and equal to 60 Å/sec . For $x \geq 10^{-3}$, the etching rate was also constant and equal to 320 Å/sec . The slow etching rates observed indicate that the films are

dense and possibly close to the theoretical density of ZnO.

Figure 5 - Scanning electron microscopy picture of a fracture edge of the ZnO film in Fig. 2.

The surface roughness of a ZnO film grown under optimum deposition conditions was measured as shown in Fig. 6. For the region where the ZnO was grown on oxidized silicon, the average surface roughness is of the order of $\pm$ 50 Å. For the region where the ZnO film was grown on diffused p⁺n diodes, the surface follows the profile of the thermal oxide grown on the p⁺ and n regions, as shown in the Lower part of Fig. 6. It is seen that the films are very smooth and should be suitable for optic and acousto-optic applications.

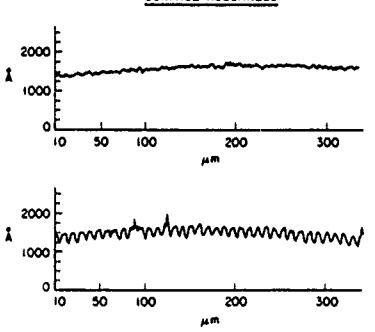

Figure 6 - Surface roughness profile of a ZnO film on SiO_2/Si and on p⁺n diode in Si.

Acoustic measurements were also used to characterize the ZnO films. A bulk wave delay line on a sapphire buffer rod is made for every ZnO run. The tuned round trip insertion loss of the delay line is measured and used to characterize the ZnO film. Table 2 summarizes the results for different delay lines on a sapphire buffer rod 2 mm long operating at different center frequencies. Again, these results indicate that the ZnO films are highly oriented. Surface wave convolvers and correlators on (111) and (100) Si substrates were made using this sputtering technique. The convolver efficiency, $F_T = P_3/P_1P_2$, where P_3 is the output power and P_1 and P_2 the input powers to the transducers, is used to characterize the ZnO films. The efficiencies obtained are the best reported to date and indicate excellent quality for the ZnO films. Table 3 summarizes these results.[5,6]

Table 2

Tuned round trip insertion loss for various bulk wave delay lines

Center Frequency (MHz)	Loss (dB)
300	3
600	5
1000	7
2000	11
4000	18

Table 3

External convolution efficiencies for various acoustoelectric convolvers

Convolver Type	Center Frequency (MHz)	F_T dBm
Rayleigh wave	125	-55
Waveguide Rayleigh wave	125	-44
Sezawa wave	160	-50

Highly oriented ZnO films are obtained using reactive sputtering of ZnO in a planar magnetron system. Very high sputtering rates (10 - 20 μm per hour) are typical, and excellent quality films are obtained on a variety of substrates. Substrate temperature control is dominated by the substrate heater, thus allowing greater control on the deposited film.

Acknowledgements

The authors would like to thank G. S. Kino for many useful discussions and J.E. Bowers, J.B. Green, and R.L. Thornton for the use of their results on SAW devices. This work has been supported by the Defense Advanced Research Projects Agency and monitored by the Office of Naval Research under Contract No. N00014-78-C-0129.

References

1. T. Yamamoto, T. Shiosaki, and A. Kawabata, J. Appl. Phys. 51(6), pp. 3113-3120, June 1980.

2. T. Hata, E. Noda, O. Morimoto, and T. Hada, Proc. IEEE Sonics and Ultrasonics Symposium, p. 936, 1979.

3. Thin Film Processes, J.L. Vossen and W. Kern, eds., Academic Press, 1978.

4. A. J. Bahr, R. E. Lee, and F. S. Hickernell, Proc. IEEE Sonics and Ultrasonics Symposium, p. 199, 1972.

5. J. B. Green, B. T. Khuri-Yakub, and G. S. Kino, Proc. IEEE Sonics and Ultrasonics Symposium, p. 911, 1979.

6. J. E. Bowers, B. T. Khuri-Yakub, and G. S. Kino, Proc. IEEE Sonics and Ultrasonics Symposium, 1980.

APPENDIX D

THE DESIGN OF BROADBAND AND EFFICIENT ACOUSTIC WAVE TRANSDUCERS

C.H. Chou, J.E. Bowers, A.R. Selfridge, B.T. Khuri-Yakub, and G.S. Kino

Edward L. Ginzton Laboratory
Stanford University
Stanford, California 94305

Abstract

The basic design criteria for SAW transducers is typically a flat frequency response. The basic design criteria for bulk wave transducers in nondestructive evaluation and medical imaging is the compactness of the impulse response. This criteria is different from the usual flat frequency response criteria because a flat bandwidth does not necessarily imply a compact impulse response. An iterative optimization program, based on a least mean square algorithm, has been developed and used to simultaneously optimize matching networks and acoustic parameters to achieve either of the above design criteria. The optimization is first illustrated in the frequency domain for an IDT transducer. Then the optimization is done in the time domain for a bulk wave transducer with the criterion of reducing the length of the impulse response. The impulse response is thus reduced from about 15 cycles to 3 cycles and has an almost Gaussian frequency response. The increase in the round trip insertion loss of the transducer due to the tuning is of the order of a few dB. Transducers have been constructed at 5 and 35 MHz with a backing of epoxy ($Z \approx 3$ kg/m^{2}sec) and no front matching layer. The agreement between theory and experiment is excellent.

1. Introduction

A number of techniques have been developed to design broadband flat frequency response matching networks[1-4] for acoustic transducers. The load is usually modeled as a resistor and capacitor[3] or as a simple four-element circuit.[4] The problem with this approach is that the frequency response of acoustic transducers has a resonance characteristic which is difficult to accurately mimic with the use of fixed component networks. In most cases, improved results can be obtained if the network suggested by one of the techniques listed in Refs. 1-5 is used as a starting point for an optimization routine which accurately takes into account the frequency dependent radiation resistance and reactance. An algorithm is developed in this paper for that purpose.

This algorithm is extremely flexible and can be used in the frequency domain or in the time domain to reduce the length of the impulse response. The use of this algorithm in the design of transducers with and without acoustic matching layers has resulted in impulse responses which are better than those obtained using any other technique.[5] In one example presented here, the impulse response of a PZT transducer operated directly into water was reduced from 15 cycles to 3 cycles with the use of a four-element optimized tuning circuit

2. Theory

Consider the system shown schematically in Fig. 1. Suppose the response of the matching network and load is $Y(\omega)$, where $Y(\omega)$ is any parameter which is to be optimized, such as voltage, current, or power. If the desired response is $D(\omega)$, then the error in the response is

$$E(\omega) = D(\omega) - Y(\omega) \qquad (1)$$

The response $Y(\omega)$ is a function of N adjustable real parameters β_n. These parameters are generally matching network parameters, such as inductance, capacitance, transistor gain, etc. This algorithm can also be used to simulateously design the transducer (load) and matching network, and in this case, the matching parameters also include transducer width, acoustic impedance, quarter wave matching layer, apodization, etc.

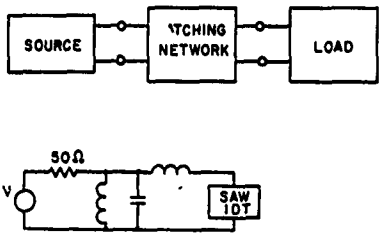

Figure 1 - Schematic drawing of source, matching network, and load.

The square error is

$$E(\omega)E^*(\omega) = [Y(\omega) - D(\omega)][Y^*(\omega) - D^*(\omega)] \qquad (2)$$

and the change in the square error due to a change $\Delta\beta_n$ is

Reprinted from 1980 ULTRASONICS SYMPOSIUM PROCEEDINGS, November 1980

0090-5607/80/0000-0984 $00.75 © 1980 IEEE

$$\frac{\partial[E(\omega)E^*(\omega)]}{\partial\beta_n} = E^*(\omega)\frac{\partial E(\omega)}{\partial\beta_n} + E(\omega)\frac{\partial E^*(\omega)}{\partial\beta_n} \quad (3)$$

$$= -2\mathrm{Re}\, E^*(\omega)\frac{\partial Y(\omega)}{\partial\beta_n} \quad (4)$$

The goal of this algorithm is to minimize the mean square error averaged over the frequency range ω_1 to ω_2, i.e. minimize ε where

$$\varepsilon = \int_{\omega_1}^{\omega_2} E(\omega)E^*(\omega)d\omega \quad (5)$$

To achieve this goal, we require that the change $\Delta\varepsilon$ for a change $\Delta\beta_n$ be negative

$$\Delta\varepsilon = \frac{\partial\varepsilon}{\partial\beta_n}\Delta\beta_n + \ldots < 0 \quad (6)$$

$$\approx -2\Delta\beta_n\,\mathrm{Re}\left[\int_{\omega_1}^{\omega_2} d\omega E^*(\omega)\frac{\partial Y(\omega)}{\partial\beta_n}\right] < 0 \quad (7)$$

There are a number of expressions that could be used to choose $\Delta\beta_n$. From Eq. (7) we see that $\Delta\varepsilon$ will be negative if we choose

$$\Delta\beta_n = \alpha_n\,\mathrm{Re}\left[\int_{\omega_1}^{\omega_2} d\omega E^*(\omega)\frac{\partial Y(\omega)}{\partial\beta_n}\right] \quad (8)$$

where α_n is a positive real constant. The change in ε is then

$$\Delta\varepsilon = -2\alpha_n\left\{\mathrm{Re}\left[\int_{\omega_1}^{\omega_2} d\omega E^*(\omega)\frac{\partial Y(\omega)}{\partial\beta_n}\right]\right\}^2 \quad (9)$$

which is negative as desired.

One of the conditions for convergence is that

$$\Delta\varepsilon < 0 \quad (10)$$

Eq. (10) will be satisfied if

$$\alpha_n = \frac{\gamma\int_{\omega_1}^{\omega_2} d\omega E(\omega)E^*(\omega)}{2\left\{\mathrm{Re}\left[\int_{\omega_1}^{\omega_2} d\omega E^*(\omega)\frac{\partial Y(\omega)}{\partial\beta_n}\right]\right\}^2} \quad (11)$$

where γ is real and $0 < \gamma < 1$. The expression for $\Delta\beta_n$ becomes

$$\Delta\beta_n = \frac{\gamma\int_{\omega_1}^{\omega_2} d\omega E(\omega)E^*(\omega)}{2\mathrm{Re}\left[\int_{\omega_1}^{\omega_2} d\omega E(\omega)\frac{\partial Y(\omega)}{\partial\beta_n}\right]} \quad (12)$$

If we consider the simple case $N = 1$ in the limit $\omega_2 - \omega_1 \to 0$, then Eq. (12) becomes

$$\Delta\beta_n = \gamma\frac{E}{\frac{dY}{d\beta}} = \gamma\frac{E}{\frac{dE}{d\beta}} \quad (13)$$

This is the familiar expression used in Newton's method for finding the zero of the function E.

In general, the surface $\varepsilon(\beta_1, \beta_2, \ldots \beta_n)$ will have a number of local minima. Thus, it is important to use an appropriate set of starting conditions β_{n0} based on simple calculations, standard design rules, and intuition. This algorithm can then be used to find the local minimum. Alternatively, a set of starting conditions can be used and then the various minima compared.

The analysis given above is the same when the independent variable is frequency, time, phase, or any other parameter. For instance, consider the case where it is desired to optimize the impulse response $Y(t)$ of a transducer. The desired response $D(t)$ could be a one cycle sinusoid. From Eq. (12), a good choice for the change in each of the components for each iteration is

$$\Delta\beta_n = \alpha\frac{\int dt E^2(t)t}{2\int dt E(t)\frac{\partial Y(t)}{\partial\beta_n}} \quad (14)$$

However, the best results were obtained when an expression based on Eq. (8) is used for $\Delta\beta_n$:

$$\Delta\beta_n = \frac{G}{\frac{\partial G}{\partial\beta_n}} \quad (15)$$

where $G = 1/S^2\int_0^\infty E(t)tdt$ and S is the impulse peak amplitude. In this case, the algorithm tries to reduce the ripple, but also maximizes the transmission. If a larger exponent of S is used, then the importance of maximum transmission is emphasized. If a smaller exponent (1) is used, then minimum ripple is emphasized.

To calculate $\Delta\beta_n$, one starts with the measured or calculated transducer response and calculates the insertion loss of the network plus load, $Y(\omega)$. The Fourier transform $Y(t)$ is determined, and $\Delta\beta_n$ is calculated from Eq. (15). Due to the additional task of calculating Fourier transforms, the optimization in the time domain typically takes longer than optimization in the frequency domain.

However, as we shall see, the impulse response obtained optimization in the time domain is significantly better.

3. Results and Discussion

SAW Devices

The use of this algorithm will first be illustrated in the design of a matching network for a SAW Sezawa wave IDT. The goal was a frequency response which is between 0 and 1.5 dB over the frequency range 146 MHz to 183 MHz . The starting parameters for the optimization are given in Table 1. The optimization results after 1, 10, 100, and 130 iterations are shown in Fig. 2. The optimization was stopped after achieving a 1.5 dB bandwidth of 36 MHz. The final values of the network components (Table 1) are all easily realizable. Limits should be placed on the possible values of the network components during optimization so that a realizable filter is obtained.

Table 1 - Values used in optimizing the matching network of a Sezawa wave IDT

IDT Parameters: $R = 250\ \Omega$, $C_T = .5$ pF , $C_p = .2$ pF, $N = 4$, $W = 1$ mm , $\Delta v/v = .028$

Matching Network Parameters:

	L_1 (μH)	L_2 (μH)	L_3 (μH)	C_1 (pF)	C_2 (pF)	C_3 (pF)
Initial	1	.1	.1	10	10	10
Final	1.35	.047	.024	8.93	17.7	68.3

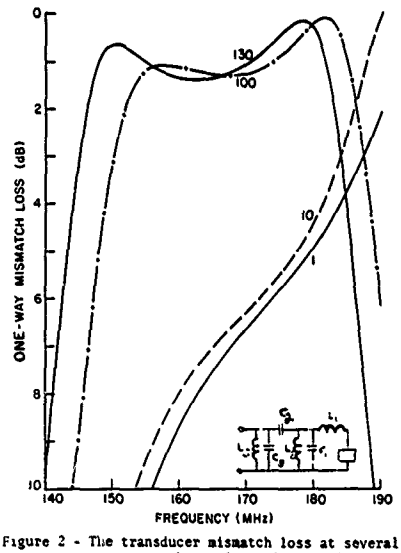

Figure 2 - The transducer mismatch loss at several points in the optimization routine

This algorithm can be used to simultaneously optimize the transducer beamwidth, number of finger pairs, finger width to spacing ratio, and apodization dependence, in addition to optimizing the values of the matching network.

Bulk Wave Transducer

The algorithm has been used to design a matching network for a longitudinal wave transducer. The transducer operates in water without any matching layers and has a lossy low impedance backing, namely epoxy with $Z_a = 3 \times 10^6$ kg/m^2-sec . Transducers have been designed and built to operate at a center frequency of 35 MHz . The transducer material used is Murata-PZT for the 35 MHz transducer. Figure 3 shows the insertion loss and impulse response of the 35 MHz transducer, where the active area is 2 mm in diameter. The design criteria used for the circuit components was a compact impulse response. A four-component matching network was designed in the configuration shown in Fig. 4. Figure 4 also shows the theoretical insertion loss and impulse response of the transducer with the proper matching network. Notice that the band shape is almost Gaussian and that the impulse response was reduced from 15 full cycles to 3 full cycles. Figure 5 shows the experimental results obtained for the transducer. The agreement between theory and experiment is excellent.

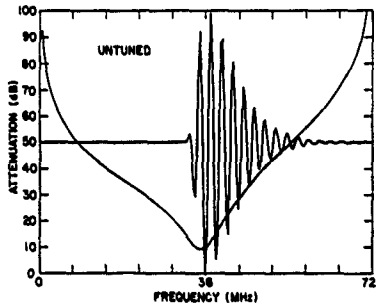

Figure 3 - Impulse response and frequency response of 35 MHz epoxy bonded PZT transducer operating into water

Bulk Wave Transducer Array

The algorithm has also been used to optimize the impulse response of the transducer elements in a linear array. Again, the design criteria used was a compact impulse response. The PZT-5H transducer elements are resonant at a center frequency of 3 MHz and have a width of 250 μm , a width-to-height ratio of 0.6 , a low impedance lossy backing $Z_a = 3 \times 10^6$ kg/m^2-sec , and one front matching layer. The optimized parameters in this case were: the transformer turn ratio (match into 50 Ω), the transformer inductance, and the length and impedance of the matching layer. Note that in this case both electrical and acoustic parameters are optimized. Figure 6 shows the insertion loss

and impulse response of an array element designed with conventional method[5] assuming a matched source, namely $f/2f_0 = .9$ where f_0 is the resonant frequency of the piezoelectric ceramic and f is the resonant frequency of the matching layer. Figure 7 shows the insertion loss and impulse response of an array element designed with our optimization program. In this case, the thickness of the matching layer was such that $f/2f_0$ was 1.37 , and the impedance of the matching layer was 4.7×10^6 kg/m^2/sec. Notice that the impulse response in Fig. 7 is greatly improved over the impulse response of Fig. 6.

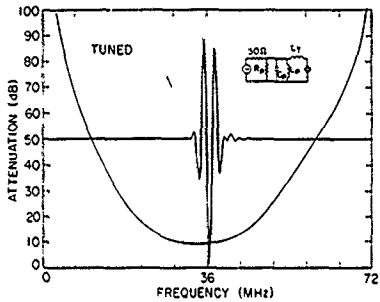

Figure 4 - Optimized impulse response and frequency response after 30 iterations

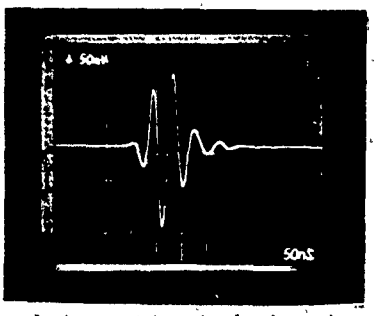

Figure 5 - Experimental results for the impulse response with and without matching network

4 Conclusion

A flexible algorithm has been developed which is important to the design of improved bulk and surface acoustic wave transducers. The impulse response of a PZT transducer operating into water was reduced from 15 cycles to 5 cycles with the use of this algorithm. The agreement between theory and experiment was excellent.

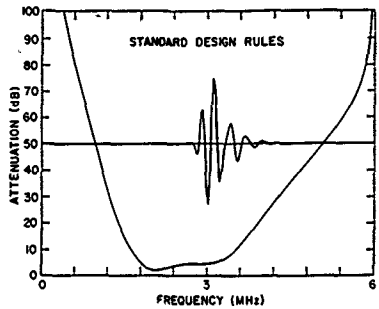

Figure 6 - Impulse response and frequency response of a 3 MHz PZT transducer with epoxy backing and a single matching layer. Standard design rules were used to obtain matching layer parameters

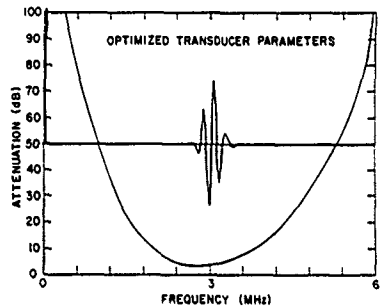

Figure 7 - Optimized impulse response and frequency response of the transducer shown in Fig. 6

Acknowledgement

This work was supported by the Air Force Office of Scientific Research under Contract No. 49620-79-C-0217, the Electric Power Research Institute under Contract No. RP609-1, the Office of Naval Research under Contract No. N00014-76-C-0129, and the Advanced Research Projects Agency under Rockwell International Subcontract No RISC-80-F01236-3

References

1 D.C. Youla, "A New Theory of Broadband Matching" IEEE Trans. Cir. Theory, vol. CT-11, p. 30, 1964

2. R.M. Fano, "Theoretical Limitations on the Broadband Matching of Arbitrary Impedances," J Franklin Institute, vol 244, p. 57 and 139, 1950.

3. T.M. Reeder, W.R. Schreve, and P.L. Adams, "A New Broadband Coupling Network for Interdigital Surface Wave Transducers," IEEE Trans. Sonics and Ultrasonics, vol. SU-19, p. 466, 1972.

4. J. Anderson and L. Wilkins, "The Design of Optimum Lumped Broadband Equalizers for Ultrasonic Transducers," J. Acous. Soc., vol. 66, p. 629, 1979.

5. C. DeSilets, J. Fraser, and G. Kino, "The Design of Efficient Broadband Piezoelectric Transducers," IEEE Trans. Sonics and Ultrasonics, vol. 25, p. 115, 1978.

DISTRIBUTION LIST

Addressee	Number of Copies
Director Advanced Research Projects Agency 1400 Wilson Boulevard Arlington, VA 22209 Attention: Program Management	1
Scientific Officer, ONR Code 427	3
Administrative Contracting Officer	1
Director Naval Research Laboratory Attention: Code 2627 Washington, DC 20375	6
Office of Naval Research Department of the Navy Arlington, VA 22217 Attention: Code 102IP	6
Defense Documentation Center Bldg. 5 Cameron Station Alexandria, VA 22314	12
Office of Naval Research, Branch Office 1030 East Green Street Pasadena, CA 91101	1
Naval Research Laboratory Code 5250 Washington, DC 20375	1
RADC (ETEM) Attn: Dr. P. Carr Hanscom AFB, MA 01731	1
AGED ODDR&E 9th Floor 201 Varick Street New York, NY 10014	1
Dr. R. Damon Director, Applied Physics Lab. Sperry Research Center Sudbury, MA 01776	1

Addressee	Number of Copies
Dr. R. S. Wagers M.S. 134 Texas Instruments P.O. Box 225936 Dallas, Texas 75265	1